

Load Testing and Load Rating
Prestressed Concrete Box Beams
Hopkins Street Bridge, Defiance County, Ohio



SUBMITTED TO:

Defiance County Engineers Office
500 Second Street
Defiance, OH 43512

BY:

BRIDGE DIAGNOSTICS, Inc.
5398 Manhattan Circle, Suite 100
Boulder, Colorado 80303-4239
(303) 494-3230

June 10, 2002

Table of Contents

| | |
|---|----|
| INTRODUCTION | 1 |
| GENERAL OVERVIEW | 1 |
| Instrumentation and Testing Procedures | 1 |
| Data Evaluation | 1 |
| Modeling and Analysis | 2 |
| Load Rating Procedures | 2 |
| Summary of Load Rating Results and Distribution Factors | 2 |
| CONCLUSIONS AND RECOMMENDATIONS | 3 |
| LOAD TEST AND EVALUATION DETAILS | 4 |
| Description of Structure | 4 |
| Instrumentation and Load Test Details | 4 |
| Preliminary Investigation of Test Results | 6 |
| Analysis and Model Calibration | 8 |
| Span A | 10 |
| Span B | 11 |
| Span C | 12 |
| Load Rating Calculations | 13 |
| Measured and Computed Strain Comparisons | 13 |
| APPENDIX A - FIELD TESTING PROCEDURES | 25 |
| Attaching Strain Transducers | 26 |
| Assembly of System | 26 |
| Performing Load Test | 27 |
| APPENDIX B - MODELING AND ANALYSIS: THE INTEGRATED APPROACH | 29 |
| Introduction | 29 |
| Initial Data Evaluation | 29 |
| Finite Element Modeling and Analysis | 30 |
| Model Correlation and Parameter Modifications | 31 |
| APPENDIX C - LOAD RATING PROCEDURES | 34 |
| APPENDIX D - REFERENCES | 37 |

List of Figures

| | |
|---|----|
| Figure 1 - Instrumentation Plan..... | 5 |
| Figure 2 Load Configuration of Test Truck..... | 5 |
| Figure 3 Reproducibility of load test procedures and structural response..... | 7 |
| Figure 4 2-D model of Defiance County Hopkins St. Bridge - Span A. | 10 |
| Figure 5 Span A – Beam 3 midspan. | 14 |
| Figure 6 Span A – Beam 4 midspan. | 14 |
| Figure 7 Span A – Beam 5 midspan. | 15 |
| Figure 8 Span A – Beam 6 midspan. | 15 |
| Figure 9 Span A – Beam 7 midspan. | 16 |
| Figure 10 Span A – Beam 3 @ west abutment..... | 16 |
| Figure 11 Span B – Beam 3 midspan. | 17 |
| Figure 12 Span B – Beam 4 midspan. | 17 |
| Figure 13 Span B – Beam 5 midspan. | 18 |
| Figure 14 Span B – Beam 6 midspan. | 18 |
| Figure 15 Span B – Beam 7 midspan. | 19 |
| Figure 16 Span B – Beam 8 midspan. | 19 |
| Figure 17 Span B – Beam 9 midspan. | 20 |
| Figure 18 Span B – Beam 10 midspan. | 20 |
| Figure 19 Span B – Beam 11 midspan. | 21 |
| Figure 20 Span B – Beam 12 midspan. | 21 |
| Figure 21 Span C – Beam 8 midspan. | 22 |
| Figure 22 Span C – Beam 9 midspan. | 22 |
| Figure 23 Span C – Beam 10 midspan..... | 23 |
| Figure 24 Span C – Beam 11 midspan..... | 23 |
| Figure 25 Span C – Beam 12 midspan..... | 24 |
| Figure 26 Illustration of Neutral Axis and Curvature Calculations | 30 |
| Figure 27 AASHTO rating and posting load configurations..... | 36 |

List of Tables

| | |
|---|----|
| Table 1 Summary of critical HS-20 rating factors (moment). | 3 |
| Table 2 Load Test Data Files..... | 6 |
| Table 3 Extreme Strain Values (micro-strain). | 7 |
| Table 4 Analysis and model details – Whatcom County High Bridge | 8 |
| Table 5 Hopkins St. Span A model calibration results. | 11 |
| Table 6 Hopkins St. Span B model calibration results. | 12 |
| Table 7 Hopkins St. Span B model calibration results. | 12 |
| Table 8 Applied load and resistance factors. | 13 |
| Table 9 Material strengths used in member rating capacities..... | 13 |
| Table 10 Moment capacities, loads and rating factors..... | 13 |
| Table 11. Error Functions..... | 32 |

Introduction

Bridge Diagnostics, Inc. was contracted by the Defiance County Engineers Office to perform load testing and load rating on a six span prestressed concrete bridge located in Defiance, Ohio. Due to severe deterioration on several exterior beams a rehabilitation project is underway to strengthen the bridge. Load testing was performed prior to the retrofit to determine what effect the deterioration has on the structural performance and capacity. The baseline rating values will also be used to provide strengthening requirements and provide a basis for comparison with the modified structure.

This report contains an overview of the load test procedures and evaluation methods along with a summary of load rating results. Specific details relating to the test results, analysis statistics, and load rating are provided in following sections. Detailed information on test procedures, analysis techniques, model calibration, and load rating are provided in the Appendices at the end of the report.

General Overview

Instrumentation and Testing Procedures

The structure was instrumented with a total of 52 strain transducers to measure the primary flexural responses throughout a representative portion of the structure. Instrumentation was limited to the three western most spans (A, B and C). The goal of the instrumentation was to provide information regarding the general live load response behavior of the structure and to provide a basis for improving the accuracy of a computer representation of the structure. All of the strain sensors were attached in a completely non-destructive manner meaning that no concrete was removed in order to expose reinforcement. All measurements were made on the surface with 3-inch long strain-sensors.

After the structure was completely instrumented, controlled load tests were performed with a three-axle dump truck with known axle weights. The truck was driven along three different prescribed lateral paths. During each truck crossing, strains were measured while the vehicle's position was monitored remotely. Tests were performed twice in each path to ensure reproducibility of the testing procedure and structural responses.

Instrumentation was performed with a two-man crew on May 22, 2002. Access to the underside of the structure was obtained with ODOT's bridge inspection vehicle. The Defiance County Engineers Office provided all access, traffic control and the loading vehicle.

Data Evaluation

All of the field data was first examined graphically to determine its quality and to provide a *qualitative* assessment of the structure's live-load response. Some of the indicators of data quality included reproducibility between identical truck crossings, elastic behavior (strains returning to zero after truck crossing), and unusual shaped responses that might indicate nonlinear behavior or possible gage malfunctions. Another useful indicator of data integrity was the symmetry of responses, when applicable. For example, strain magnitudes should be similar between symmetrically placed gages and symmetrical truck paths.

In addition to a data "quality check", information obtained during the preliminary investigation was used to determine appropriate modeling procedures for support conditions and model geometry. For example any continuity in responses between spans would affect the model geometry and/or load configurations.

It should be noted that this qualitative investigation of the data is very important for establishing the direction that the quantitative investigation should take.

Modeling and Analysis

The next phase of the investigation was to develop a representative finite element model for the superstructure. As with most beam type bridges, the bridge was modeled as a 2-D grid consisting of beam, plate, and spring elements. Once the model was developed, the load testing procedures that were used in the field could essentially be "reproduced" through software. A two-dimensional "footprint" of the loading vehicle was applied to the model along the same paths that the actual test vehicle crossed the bridge. A direct comparison of strain values was then made between the analytical predictions and the experimentally measured results. The initial model was "calibrated" by modifying various properties and boundary conditions until the results matched those measured in the field. The calibration process involved changing beam stiffness, transverse member stiffness, support conditions, and connectivity between the spans. Specific details related to this bridge are presented in the following sections and the overall approach is discussed in further detail in Appendix B.

Load Rating Procedures

The goal of producing an accurate model was to obtain the ability to predict the actual structure's behavior when subjected to the design or rating loads. This approach is essentially identical to standard load rating procedures, except that a "field verified" model is used rather than a typical beam analysis combined with load distribution factors.

Rating factors were computed for moment using the AASHTO Load Factor Rating (LFR) specifications for computing Inventory and Operating Load Limits. Moment capacities were computed using AASHTO specifications for prestressed concrete members. Capacities at various sections were modified by the presence of deterioration based on information provided by the University of Dayton.

Based on the roadway width of 30 feet – three 10' wide lanes were utilized for truck placement in the load rating procedures and the calculation of wheel load distribution factors. Multiple lane load scenarios were applied using the principle of superposition.

Summary of Load Rating Results and Distribution Factors

Following are summaries of the HS-20 vehicle load rating factors for the three tested spans. Table 1 contains the critical LFD moment ratings.

Table 1 Summary of critical HS-20 rating factors (moment).

| Span | LFD-Inventory | LFD-Operating | Critical component |
|--------|---------------|---------------|------------------------|
| Span A | 1.01 | 1.68 | South Exterior Beam 10 |
| Span B | 0.58 | 0.97 | South Exterior Beam 10 |
| Span C | 1.18 | 1.96 | North Interior Beam 2 |

Conclusions and Recommendations

Conclusions made directly from the load test data are qualitative in nature. All strain measurements indicated that the structure was behaving linearly with respect to load magnitude (truck position) and all responses were elastic.

The largest strains were typically measured at midspan of the exterior beams, where the deterioration was greatest. At Span B the largest strains were obtained from Beam 2, which was adjacent to the deteriorated edge beam. Relatively large strains on the exterior beams were expected due to the deterioration and the fact that these members were loaded directly by the truck wheel loads. The fact that the adjacent beams, which were not loaded directly, also experienced as high or higher strains than the exterior beams suggest that the deteriorated edge beams have lost stiffness. The adjacent beams must therefore carry additional load.

Efforts were successful in calibrating 2-D finite element models to reproduce the measured strains with a high degree of accuracy (typical for PS/C structures). The fact that the analysis could reproduce the measured results further indicates that all responses were linear-elastic. The steps, required to obtain a good correlation, included solving for the relative stiffness between the interior beams and the deteriorated edge beams. It was also necessary to modify a number of other parameters such as effective diaphragms stiffness and beam end-restraint.

While the primary goal was to determine the effect of the deterioration on the structure's response behavior and capacity, it was determined that other factors had as much or more effect on the structure's response behavior. In general it was observed that the lateral load transfer ability of each span was somewhat irregular compared to a typical beam/slab type bridge. Since there was no slab on the adjacent box beams, the majority of load transfer was provided by the staggered diaphragms and friction between the beams. The effective stiffness of the transverse diaphragms varied significantly from span to span. It appeared that both Span A and Span B had regions along the centerline of the bridge where the lateral load transfer was nearly zero - loads applied to the north side of the bridge have little effect on the south side of the bridge and visa versa.

Some variation in beam stiffness due to deterioration was observed and quantified, however, the largest factor affecting the load rating was the assumed loss of beam capacity based on the visual inspection by University of Dayton. As long as the beams remain in a prestressed condition (net compression) the effect of deteriorated strands is much greater on the beam capacity compared to the beam's stiffness. The calculated member capacity was based strictly on the indicated loss of prestressing strands.

The load rating factors and conclusions presented in this report are provided as recommendations based on the structure's response behavior and condition at the time of load testing. Any structural degradation must be considered in future load ratings. Note that no effort was made to assess the condition or capacity of the substructure elements such as the abutments or piers.

Load Test and Evaluation Details

Description of Structure

| | |
|--------------------------|---|
| Structure Identification | Def-Hopkins Street Bridge |
| Location | Defiance, Ohio |
| Structure Type | Prestressed concrete beams with asphalt roadway |
| Span Length(s) | 79'-5", 80'-10 1/4", 94'-9 1/4", 94'-9 1/4", 80'-9 1/4", 80'-0 1/8" |
| Skew | Span A (13°), Span B (12°), Span C-F (10°) |
| Structure/Roadway Widths | 30'-0" |
| Number of Beams | 10 beams @ 3'-0 o.c. |
| Deck | Asphalt roadway deck. Depth of 2 1/2" indicated by plans. Actual depth of roadway not field verified. |
| Visual condition | Majority of beams appear to be in good condition. Severe deterioration located on outer edge of exterior beams where water and salt drain from the roadway. |

Instrumentation and Load Test Details

| | |
|----------------------------|--|
| Date | May 22, 2002 |
| Structural Reference Point | X=0, Y= 0 at northwest corner of outside edge of sidewalk beam. X direction parallel to roadway. |
| Test vehicle direction | East bound for all tests (Positive X direction). |
| Start of data recording | Data acquisition began with front axle at X = -15.25 |
| Truck position | Record truck position at every wheel revolution (10.5'). <i>Autoclicker</i> placed on driver side front wheel. |
| Lateral truck path(s) | 3 truck paths were defined for the load test. The Y position refers to distance between driver side front wheel and Structural Reference Point (Y= 0). Y1 = 9.10' Driver side wheel line Y2 = 18.50' Driver side wheel line Y3 = 35.15' Passenger side wheel line |
| Measurements | 52 strain gages recorded at 40 Hz |
| Gage Placement | See Figure 1. |
| Gage types | BDI Intelliducers |
| Number of test cycles | Data was recorded while the test truck crossed the bridge at crawl speed (5 mph). Each truck path was run twice to check reproducibility. |

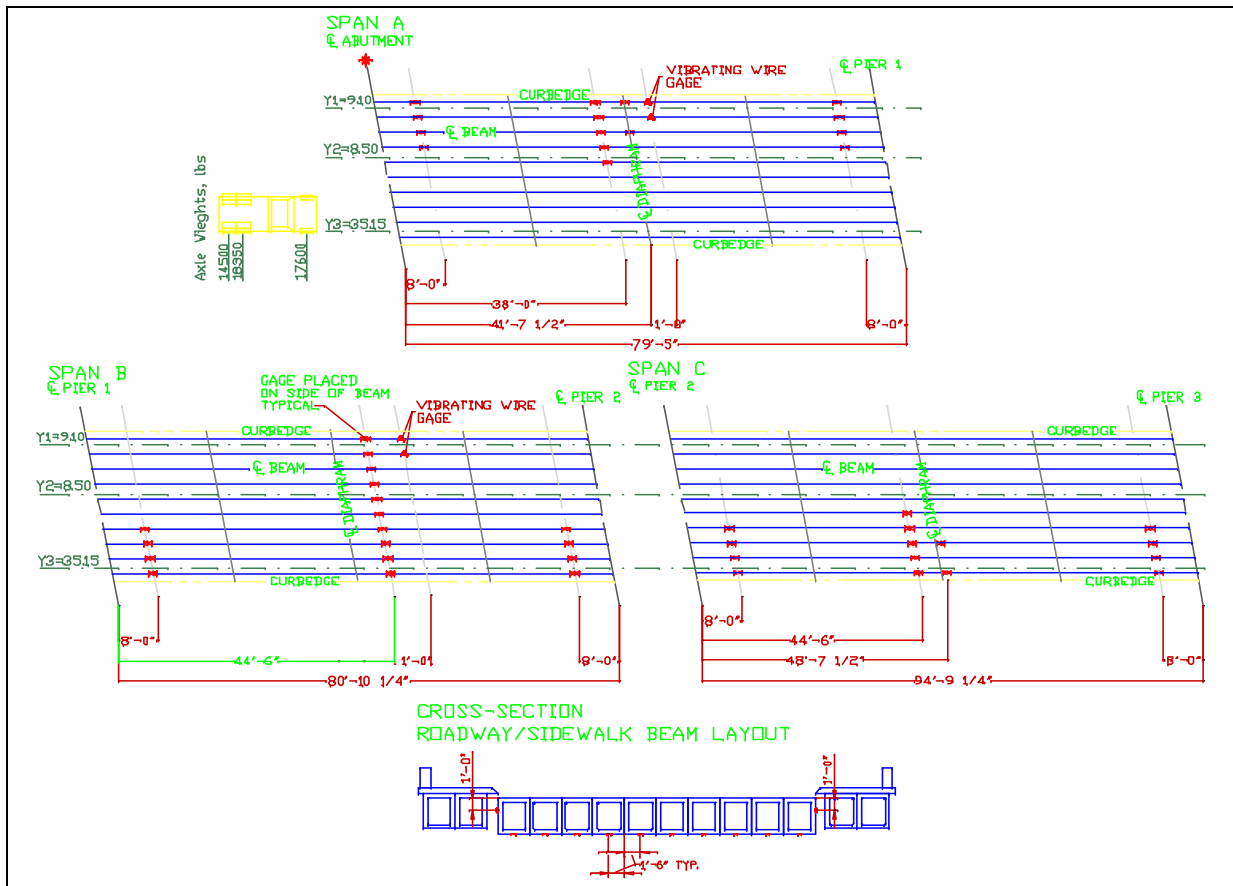


Figure 1 - Instrumentation Plan.

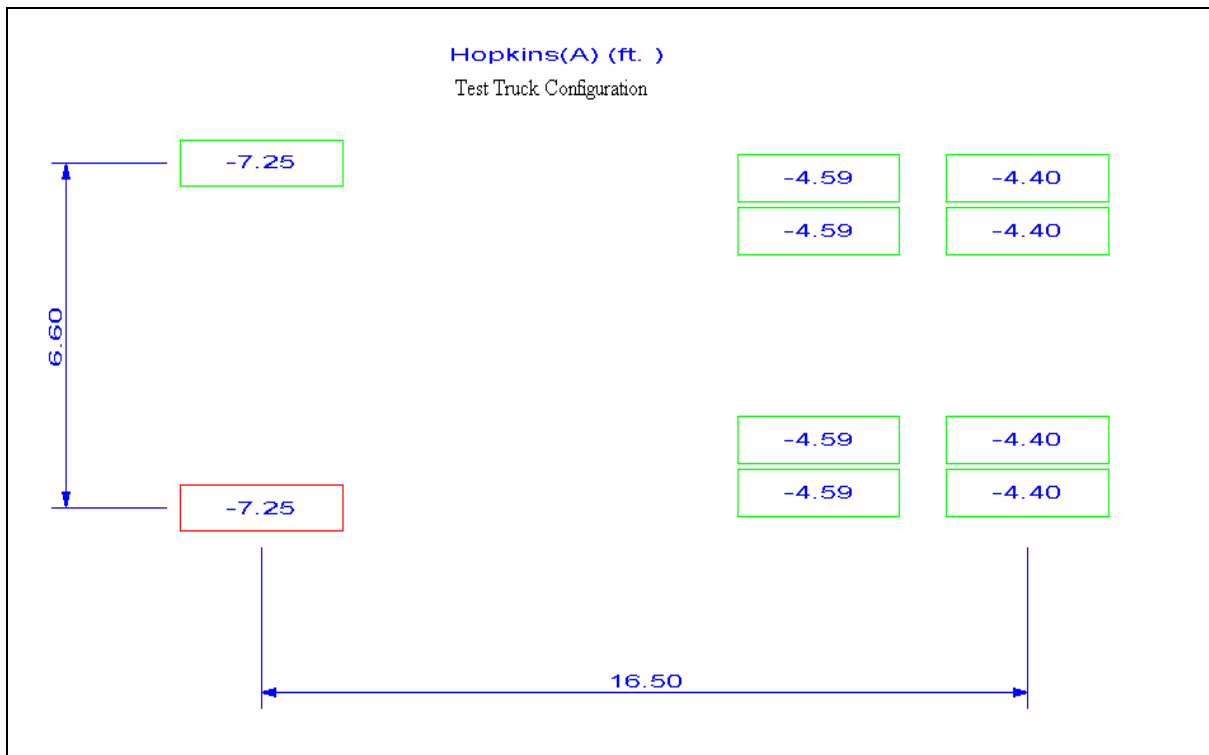


Figure 2 Load Configuration of Test Truck.

Table 2 Load Test Data Files

| Truck Path | STS Data File | Comments |
|------------|---------------|-------------------------------------|
| Y1 | defhop_1.dat | Driver-side wheels on Y1 (5 mph) |
| Y1 | defhop_2.dat | Driver-side wheels on Y1 (5 mph) |
| Y2 | defhop_3.dat | Driver-side wheels on Y2 (5 mph) |
| Y2 | defhop_4.dat | Driver-side wheels on Y2 (5 mph) |
| Y3 | defhop_5.dat | Passenger-side wheels on Y3 (5 mph) |
| Y3 | defhop_6.dat | Passenger-side wheels on Y3 (5 mph) |

Preliminary Investigation of Test Results

A visual examination of the field data was performed to assess the quality of the data and to make a qualitative assessment of the bridge’s live-load response. Conclusions made directly from the field data were:

- Responses from identical truck paths were very reproducible. This was true for all three spans as shown Figure 3.
- All of the strains indicated linear behavior with respect to load magnitude (truck position) and all strains returned to zero indicating elastic behavior.
- Very little continuity between spans was observed such that each span can be analyzed separately.
- For each span the maximum strains occurred at midspan of the exterior beam or at the beam adjacent to the exterior beam. The truck paths producing the largest strain values were approximately 2 feet from the curbs.
- The maximum measured (live-load) strain was 39 micro-strain which corresponds to a stress of approximately 195 psi (assuming a modulus of 5000 ksi for the PS concrete). Extreme strain values measured from each gage and truck path are provided in Table 3.

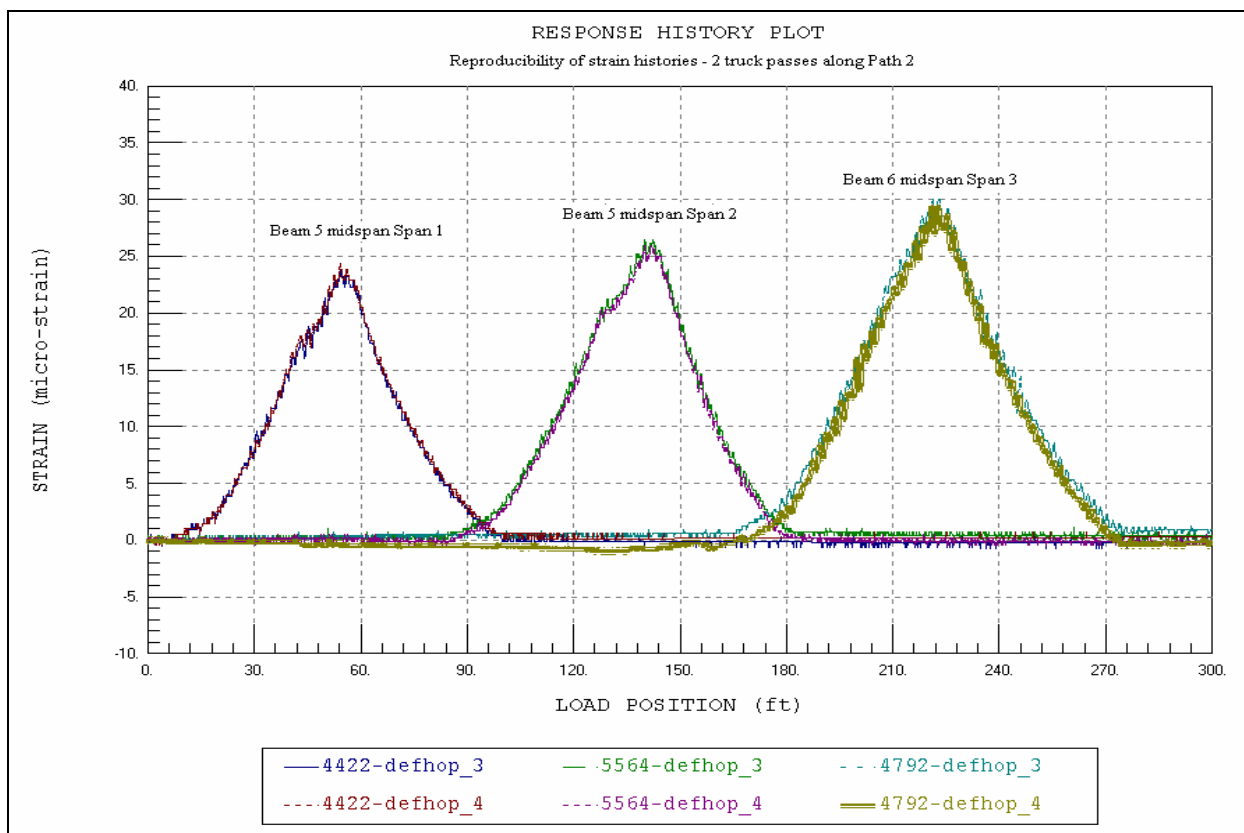


Figure 3 Reproducibility of load test procedures and structural response.

Table 3 Extreme Strain Values (micro-strain).

| Gage ID | Location | Path 1 | | Path 2 | | Path 3 | |
|---------|----------------------------------|--------|-------|--------|-------|--------|-------|
| | | min | max | min | max | min | max |
| 3872 | SpanA-BM3 Abutment | -0.23 | 17.24 | -0.76 | 2.61 | -0.54 | 1.42 |
| 3934 | SpanA-BM3 Midspan (Bottom Gage) | 0.00 | 33.96 | -0.47 | 17.06 | -1.51 | 10.10 |
| 4427 | SpanA-BM3 Midspan (Top Gage) | -16.96 | 0.12 | -7.98 | 2.77 | -4.95 | 0.00 |
| 4795 | SpanA-BM3 Midspan Diaphragm | -0.25 | 32.91 | -0.33 | 18.14 | -1.82 | 10.87 |
| 4371 | SpanA-BM3 Pier1 | -0.10 | 16.06 | -0.44 | 6.04 | -2.29 | 4.01 |
| 5854 | SpanA-BM4 Abutment | -0.12 | 14.37 | -1.27 | 3.97 | -0.69 | 2.10 |
| 4954 | SpanA-BM4 Midspan | -0.16 | 31.89 | -0.74 | 18.63 | -1.59 | 10.40 |
| 4674 | SpanA-BM4, Pier1 | -0.35 | 9.20 | -0.27 | 6.67 | -2.03 | 4.50 |
| 5562 | SpanA-BM5, Abutment | -0.19 | 16.60 | -0.97 | 5.08 | -0.64 | 2.29 |
| 4955 | SpanA-BM5, Midspan | -3.38 | 30.01 | -2.91 | 19.32 | -2.91 | 10.10 |
| 4718 | SpanA-BM5, Midspan Diaphragm | -0.71 | 30.91 | -0.64 | 20.55 | -2.69 | 10.66 |
| 5852 | SpanA-BM5, Pier1 | -0.26 | 10.69 | -0.44 | 7.21 | -1.91 | 4.55 |
| 5695 | SpanA-BM6, Abutment | -0.26 | 12.27 | -0.65 | 10.07 | -0.91 | 1.12 |
| 4050 | SpanA-BM6, Midspan | -0.39 | 28.15 | -0.63 | 21.17 | -2.37 | 10.20 |
| 4053 | SpanA-BM6, Pier1 | 0.00 | 7.42 | -0.28 | 10.25 | -1.86 | 5.65 |
| 4422 | SpanA-BM7, Midspan | -0.60 | 15.94 | -0.16 | 23.30 | -2.91 | 11.97 |
| 5692 | SpanB-BM3, Midspan (Bottom Gage) | -0.19 | 37.47 | -0.64 | 18.33 | -0.64 | 13.02 |
| 5698 | SpanB-BM3, Midspan (Top Gage) | -12.37 | 1.08 | -5.34 | 3.13 | -4.91 | 1.11 |
| 4111 | SpanB-BM4, Midspan | -0.15 | 39.10 | -0.64 | 20.75 | -0.48 | 14.31 |
| 5856 | SpanB-BM5, Midspan | -0.20 | 30.46 | -0.58 | 18.82 | -0.52 | 12.97 |
| 5853 | SpanB-BM6, Midspan | 0.00 | 22.49 | 0.00 | 25.88 | -0.33 | 16.26 |
| 5564 | SpanB-BM7, Midspan | -0.24 | 20.64 | -0.26 | 26.07 | -0.31 | 15.44 |
| 4192 | SpanB-BM8, Midspan | -0.65 | 14.65 | 0.00 | 24.61 | -0.87 | 21.35 |

| | |
|------------------|---|
| Nodal locations | <ul style="list-style-type: none"> • Nodes placed at beam bearing locations. • Longitudinal nodal placement along beams controlled by diaphragm locations. • Additional nodes spaced equally between each interval to maintain a maximum beam element length of $1/24^{\text{th}}$ of the span length. |
| Model components | <ul style="list-style-type: none"> • Asphalt represented by rectangular plate elements. • Beam elements for prestressed concrete beams. • Elastic spring elements used to simulate potential end-restraint. |
| Live-load | 2-D footprint of test truck consisting of 10 vertical point loads. Truck paths simulated by series of load cases with truck moving at 3-foot increments. |
| Dead-load | Self-weight of structure plus 37.5 lbs./ft^2 applied to the deck to account for 3" of asphalt. (Used for load rating only) |
| Data comparison | <p>Span A: 14 strain gage locations defined on model. 15 truck positions along each path. 3 truck paths (Y1, Y2, Y3) $14 \times 15 \times 3 = 630$ strain values.</p> <p>Span B: 20 strain gage locations defined on model. 15 truck positions along each path. 3 truck paths (Y1, Y2, Y3) $20 \times 15 \times 3 = 900$ strain values.</p> <p>Span C: 16 strain gage locations defined on model. 18 truck positions along each path. 3 truck paths (Y1, Y2, Y3) $16 \times 18 \times 3 = 864$ strain values.</p> <p>Strain records extracted from load test data files corresponding to analysis truck positions.</p> |

| | |
|---|---|
| Model statistics | <p>Span A</p> <p>324 Nodes 667 Elements 9 Cross-section/Material types 45 Load Cases 14 Gage locations</p> <p>Span B</p> <p>324 Nodes 667 Elements 22 Cross-section/Material types 45 Load Cases 20 Gage locations</p> <p>Span C</p> <p>324 Nodes 667 Elements 8 Cross-section/Material types 54 Load Cases 16 Gage locations</p> |
| Adjustable parameters for model calibration | <p>1 Effective Beam Stiffness (E_c - ksi).</p> <p>2 Effective stiffness of deteriorated beams ($I_x - in^4$)</p> <p>3 Transverse stiffness - diaphragms ($I_x - in^4$)</p> <p>4 Axial spring stiffness of east beam bearing ($K_x - k/in$)</p> <p>5 Axial spring stiffness of west beam bearing ($K_x - k/in$)</p> |

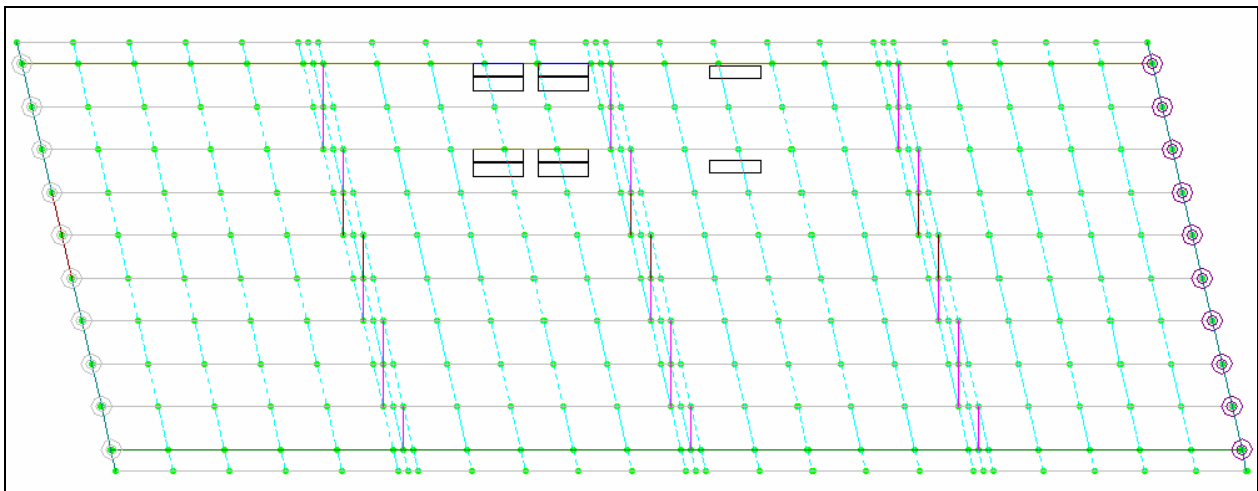


Figure 4 2-D model of Defiance County Hopkins St. Bridge - Span A.

Three models with the above parameters were defined and the analysis program simulated the load testing process. The model accuracies were defined by comparing the computed and measured strain values. Selected parameters were modified to minimize the comparison error. Following are outlines for each span that include steps taken to obtain the best correlation between the computed and measured responses.

Span A

The instrumentation plan applied to Span A was designed for Span D so unfortunately the strain transducers were concentrated on the North side of the bridge whereas the majority of deterioration on Span A was located on the South side. Results from the data comparison and parameter process indicated:

- North exterior beam had approximately the same stiffness as the interior beams
- Slight but measurable end-restraint was observed at both ends of the span
- Lateral load transfer was not consistent across the bridge. There appeared to be a reasonable degree of load transfer among the instrumented beams, however there was little load transfer from north to south sides of the bridge. It appeared that the diaphragms and shear connection between beams had failed along at least one beam line near the centerline of the bridge.
- There was no effort made to solve for the stiffness of exterior Beam 3 since instrumentation was not applied to that beam.
- Table 5 contains a comparison of stiffness parameters and error values between the initial and final model.

Table 5 Hopkins St. Span A model calibration results.

| Stiffness Parameter | Units | Initial Value | Final Value |
|------------------------------------|-----------------|---------------|-------------|
| Beam concrete (E) | ksi | 3600 | 6750 |
| Ext. Beam (I) | in ⁴ | 155300 | 155300 |
| West end-restraint spring (Kx) | k-in | 0 | 831 |
| East end-restraint spring (Kx) | K-in | 0 | 5 |
| Diaphragm stiffness (I) | in ⁴ | 198000 | 30870 |
| Diaphragm @ Beam 7 (I) | in ⁴ | 198000 | 520 |
| End diaphragm torsion (J) | in ⁴ | 150000 | 61610 |
| End diaphragm @ Beam 7 torsion (J) | in ⁴ | 150000 | 5 |
| Statistical Accuracy Values | | | |
| Absolute Error | μ€ | 5239 | 540 |
| Percent Error | % | 162 | 2.3 |
| Scale Error | % | 23 | 2.6 |
| Correlation Coefficient | | 0.928 | 0.991 |

Span B

Results from the data comparison and parameter process indicated:

- North and south exterior beams were less stiff than the interior beams. North Beam stiffness being less than the south beam stiffness even though deterioration map indicates worse deterioration at south side.
- End restraint was greater on west side than east side but varied from beam-to-beam.
- Lateral load transfer was significantly less than initially predicted.
- Large strains on Beam 4 indicate a localized region with higher flexibility may exist near midspan. Load transfer characteristics indicate that Beam 4 as a whole is relatively stiff.
- Table 6 contains a comparison of stiffness parameters and error values between the initial and final model.

Table 6 Hopkins St. Span B model calibration results.

| Stiffness Parameter | Units | Initial Value | Final Value |
|--------------------------------|-----------------|---------------|-------------|
| Beam concrete (E) | ksi | 3600 | 6561 |
| Ext. Beam 3 (I) | in ⁴ | 155300 | 121400 |
| Ext. Beam 12 (I) | in ⁴ | 155300 | 148500 |
| Beam 4 @ midspan | in ⁴ | 155300 | 119000 |
| West end-restraint spring (Kx) | k-in | 0 | varies |
| East end-restraint spring (Kx) | K-in | 0 | 62.2 |
| Diaphragm stiffness (I) | in ⁴ | 173000 | 3893 |
| End diaphragm torsion (J) | in ⁴ | 173000 | 57430 |
| Statistical Accuracy Values | | | |
| Absolute Error | με | 7358 | 529 |
| Percent Error | % | 190 | 0.9 |
| Scale Error | % | 27 | 1.5 |
| Correlation Coefficient | | 0.896 | 0.995 |

Span C

Results from the data comparison and parameter process indicated:

- The instrumented edge beam was slightly more flexible than the interior beams.
- Relatively small end-restraint was observed.
- Lateral load transfer was less than initially predicted and it appeared that the a region near the centerline of the bridge (near Beam 7) had essentially no load transfer. Loads applied to right north side of bridge do not transfer to the south side and vice versa.
- Table 7 contains a comparison of stiffness parameters and error values between the initial and final model.

Table 7 Hopkins St. Span B model calibration results.

| Stiffness Parameter | Units | Initial Value | Final Value |
|----------------------------------|-----------------|---------------|-------------|
| Beam concrete (E) | ksi | 3600 | 6950 |
| Ext. Beam 3 (I) | in ⁴ | 155300 | 139760 |
| Ext. Beam 12 (I) | in ⁴ | 155300 | 139760 |
| West end-restraint spring (Kx) | k-in | 0 | 250 |
| East end-restraint spring (Kx) | K-in | 0 | 150 |
| Diaphragm stiffness (I) | in ⁴ | 173000 | 8332 |
| Diaphragm stiffness @ Beam 7 (I) | in ⁴ | 173000 | 100 |
| Statistical Accuracy Values | | | |
| Absolute Error | με | 2775 | 985 |
| Percent Error | % | 23.0 | 3.5 |
| Scale Error | % | 14.9 | 2.1 |
| Correlation Coefficient | | 0.976 | 0.983 |

Results from all 3 spans indicate that the beam concrete modulus is higher than reasonable. It is likely that the actual wall thickness of the box beams is greater than indicated by the plans resulting in greater section properties (I).

Load Rating Calculations

Load rating factors were computed for moment responses using the AASHTO Load Factor (LFD) method. Load and resistance factors used for each rating method are listed in Table 8. The calibrated model was used to compute all live and dead load effects, except that the end-restraints were eliminated since they were not likely to be reliable.

Table 8 Applied load and resistance factors.

| Load/Resistance Factor | AASHTO LFD Inventory | AASHTO LFD Operating |
|---------------------------------|----------------------|----------------------|
| Moment Resistance Φ_M | 1.0 | 1.0 |
| Live-load factor | 2.17 | 1.30 |
| Dead-load factor | 1.30 | 1.30 |
| Impact Factor (80' / 95' spans) | 0.244 / 0.227 | 0.244 / 0.227 |

Table 9 Material strengths used in member rating capacities.

| Material | Strength value |
|----------|---|
| Steel | $f'_s = 270$ ksi |
| Concrete | $f'_c = 4000$ psi (this is likely conservative) |

Table 10 Moment capacities, loads and rating factors.

| Section | # of missing strands | ϕM_n kip-in | Dead Load Moment (Kip-in) | HS-20 Moment (Kip-in) | Rating Factors Inventory/Operating |
|-------------------|----------------------|-------------------|---------------------------|-----------------------|------------------------------------|
| Span A – Beam 1 | 0 | 24605 | 9306 | 3573 | 1.30 / 2.16 |
| Span A – Beam 2-9 | 0 | 24605 | 9949 | 3879 | 1.11 / 1.86 |
| Span A – Beam 10 | 4 | 18859 | 8024 | 3102 | 1.01 / 1.68 |
| Span B – Beam 1 | 3 | 20317 | 7801 | 2973 | 1.27 / 2.12 |
| Span B – Beam 2-9 | 0 | 24605 | 10500 | 3876 | 1.05 / 1.75 |
| Span B – Beam 10 | 5 | 17386 | 9828 | 3759 | 0.58 / 0.97 |
| Span C – Beam 1 | 1 | 30864 | 12050 | 4108 | 1.39 / 2.31 |
| Span C – Beam 2-9 | 0 | 32194 | 13480 | 4674 | 1.18 / 1.96 |

All of the critical HS-20 moment values were generated by the three-lane-load combination. A load reduction factor of 10% has already been applied to the above HS-20 moment values.

Measured and Computed Strain Comparisons

While statistical terms provide a means of evaluating the relative accuracy of various modeling procedures or help determine the improvement of a model during a calibration process, the best conceptual measure of a model's accuracy is by visual examination of the response histories. The following graphs contain measured and computed strain histories from each truck path. In each graph the continuous lines represent the measured strain at the specified gage location as a function of truck position as it traveled across the bridge. Computed stresses are shown as markers at discrete truck intervals. The three sets of data for each gage represent the three different truck paths.

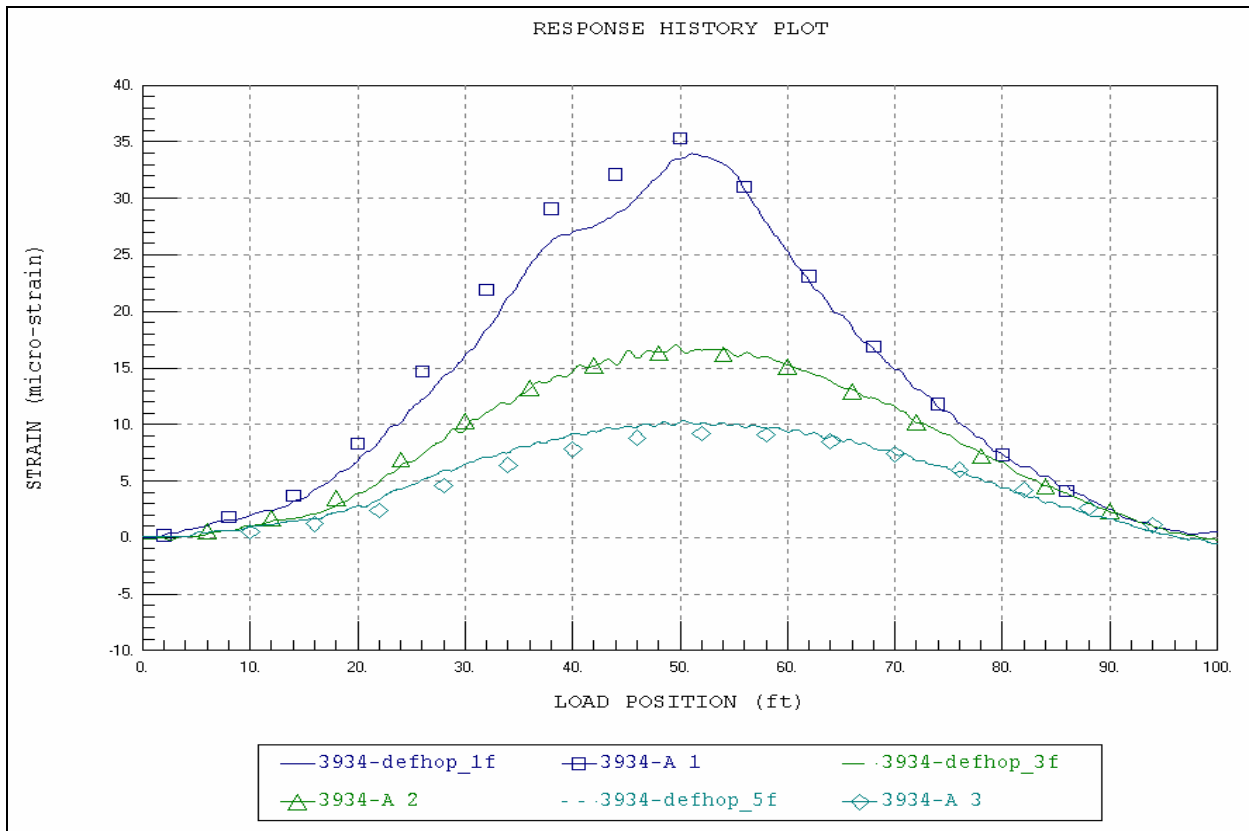


Figure 5 Span A – Beam 3 midspan.

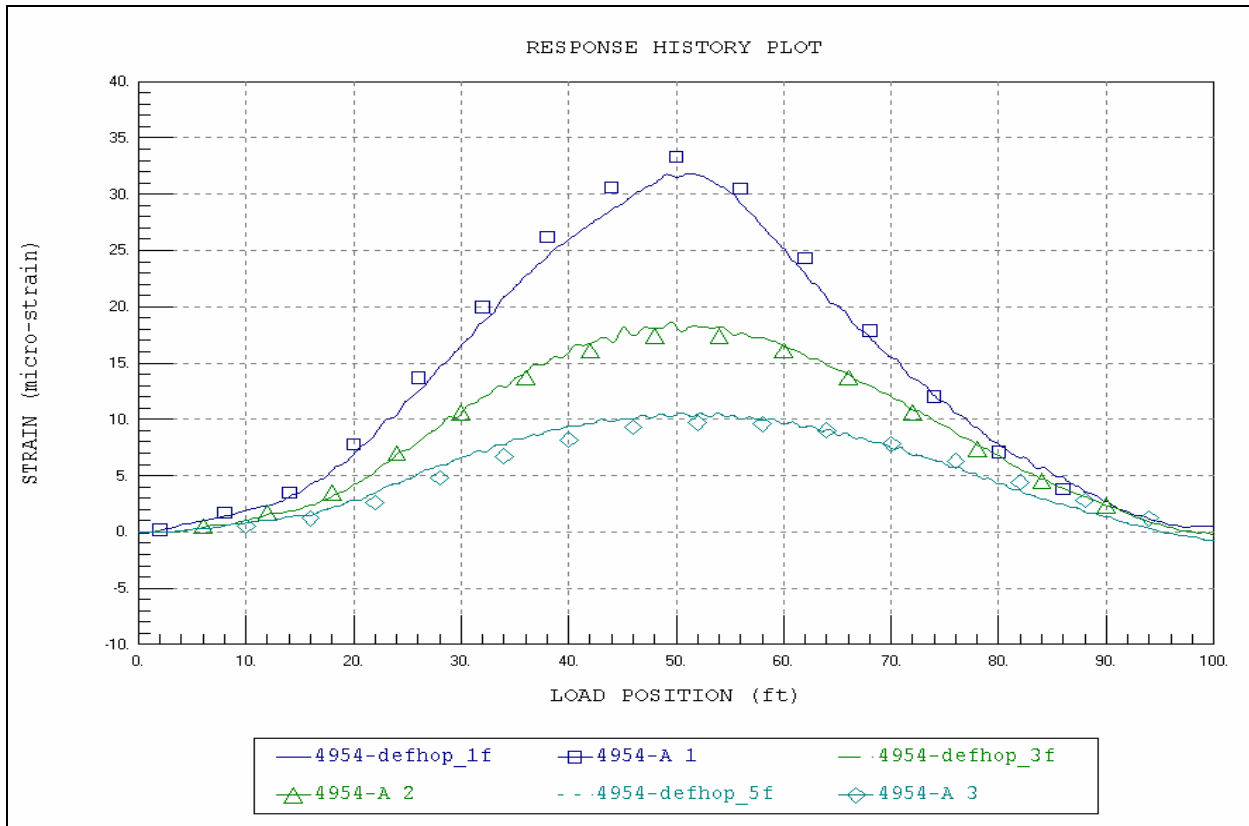


Figure 6 Span A – Beam 4 midspan.

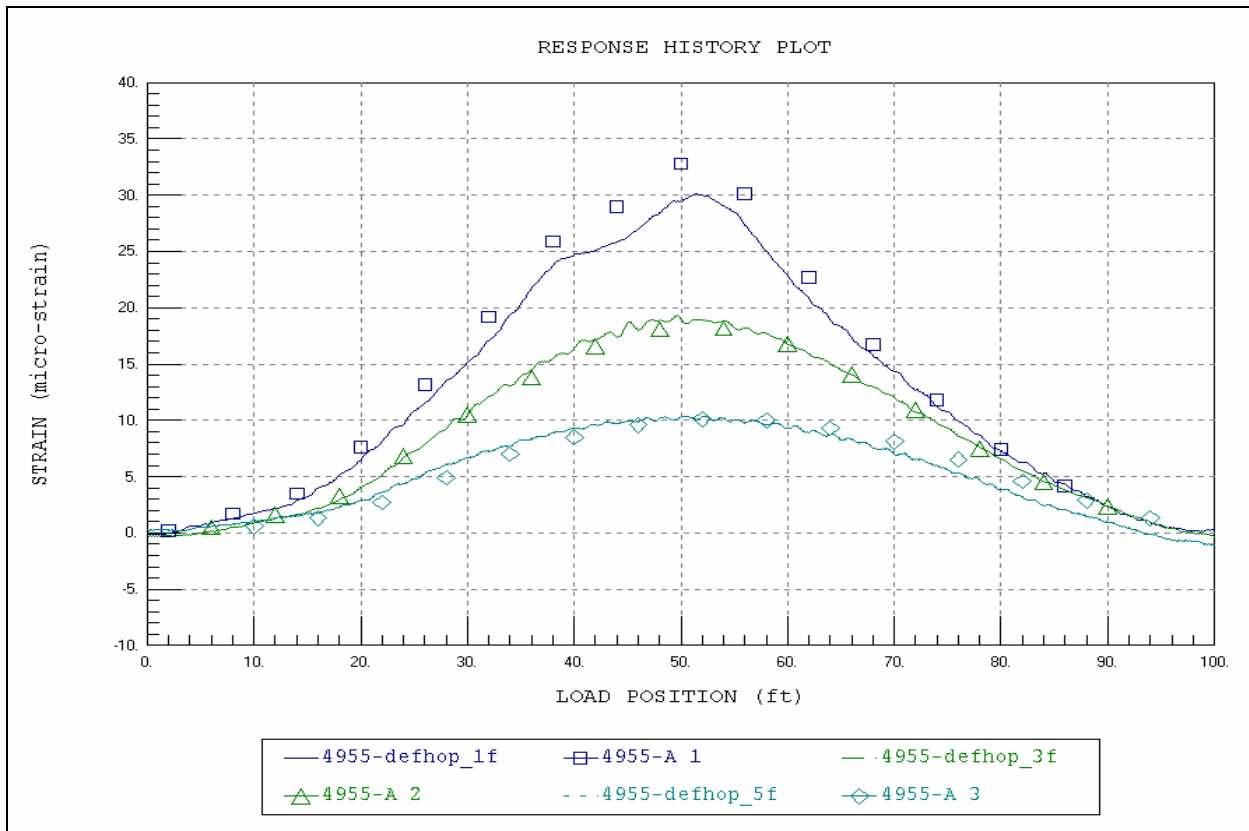


Figure 7 Span A – Beam 5 midspan.

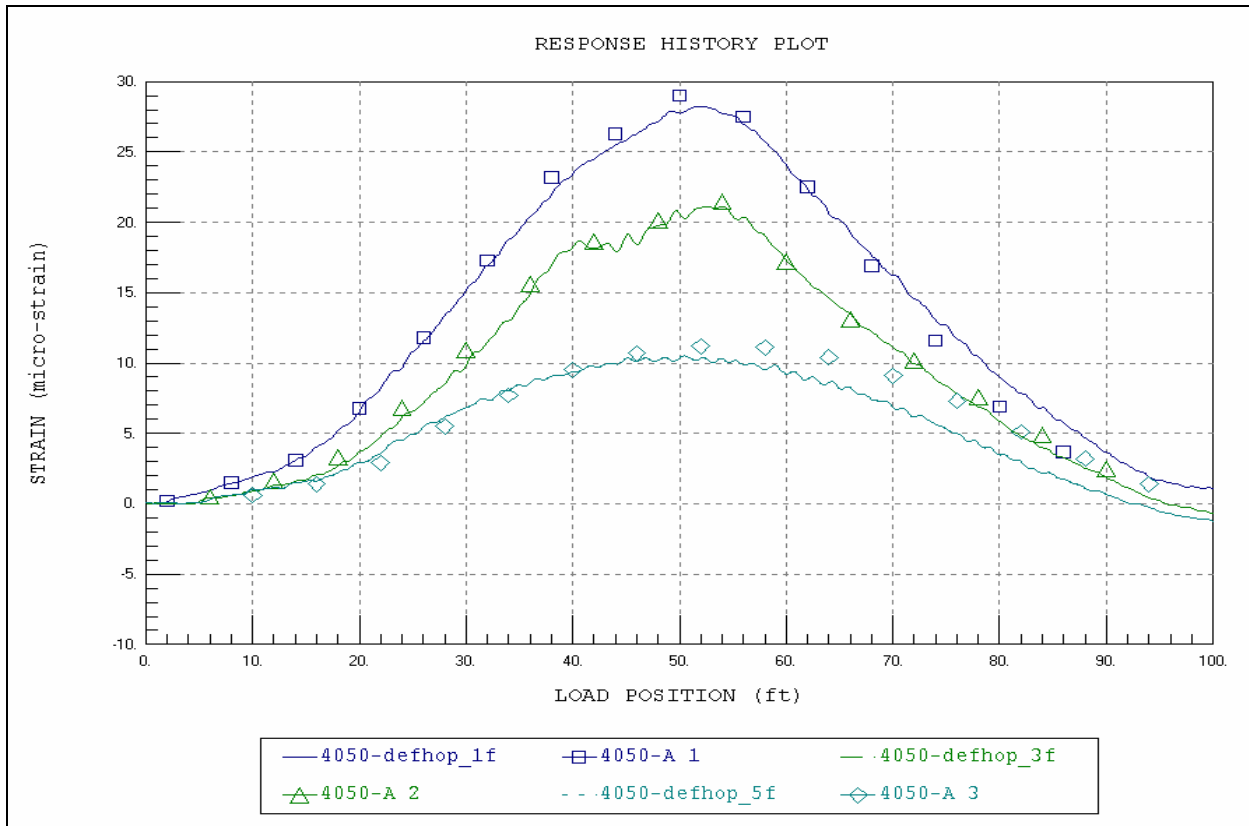


Figure 8 Span A – Beam 6 midspan.

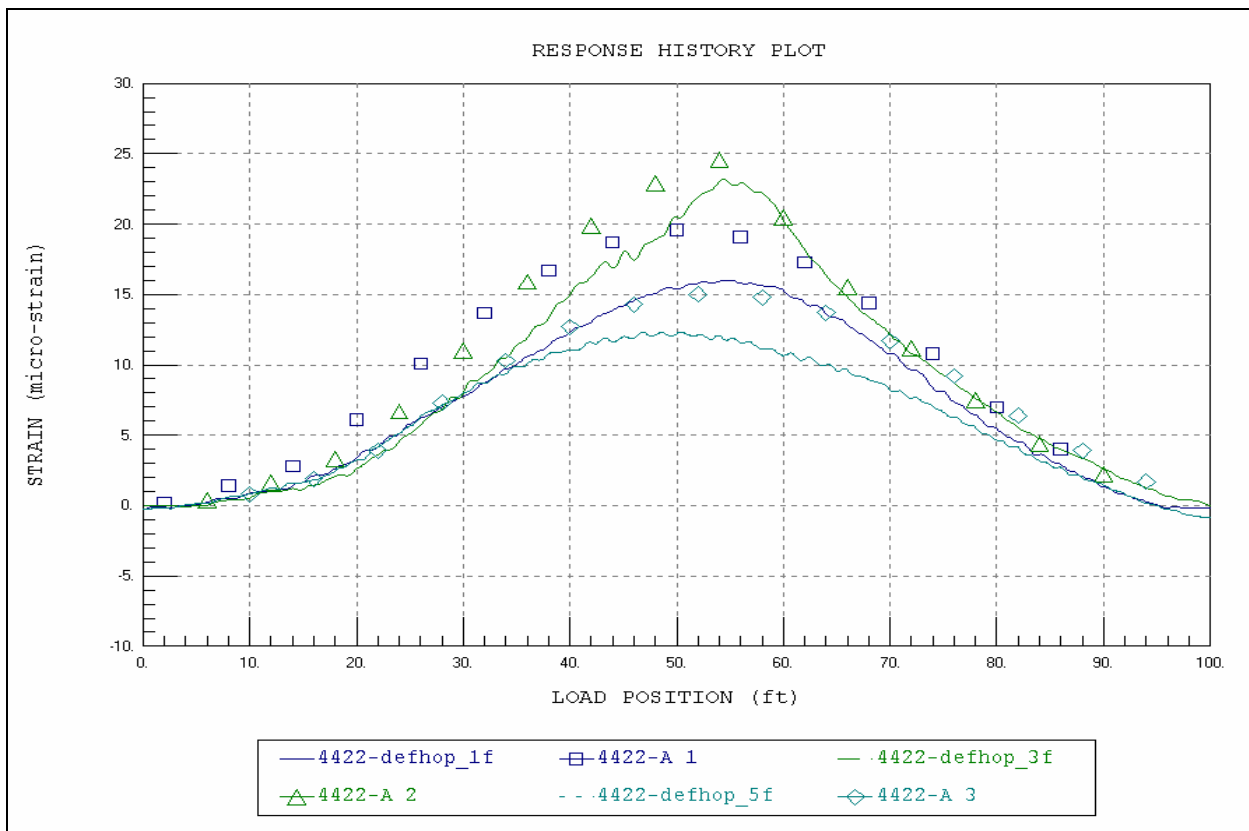


Figure 9 Span A – Beam 7 midspan.

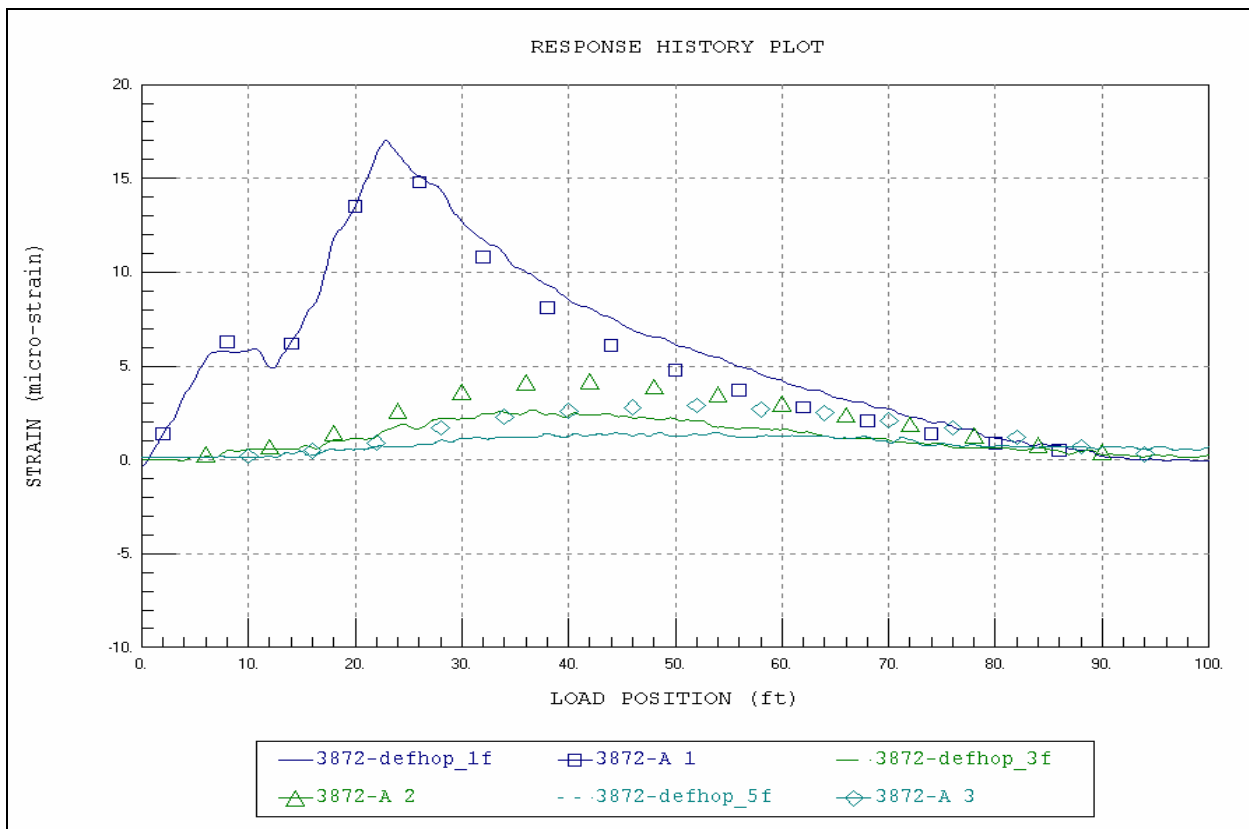


Figure 10 Span A – Beam 3 @ west abutment.

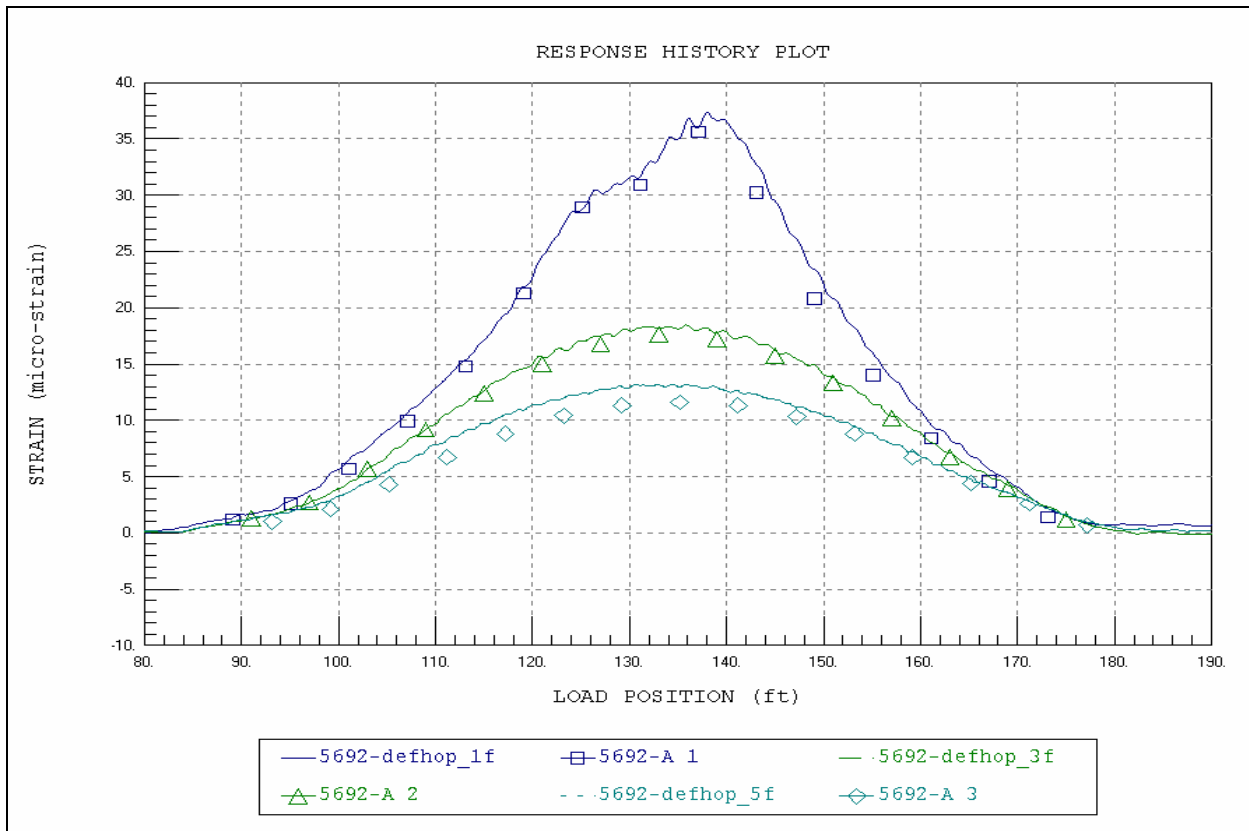


Figure 11 Span B – Beam 3 midspan.

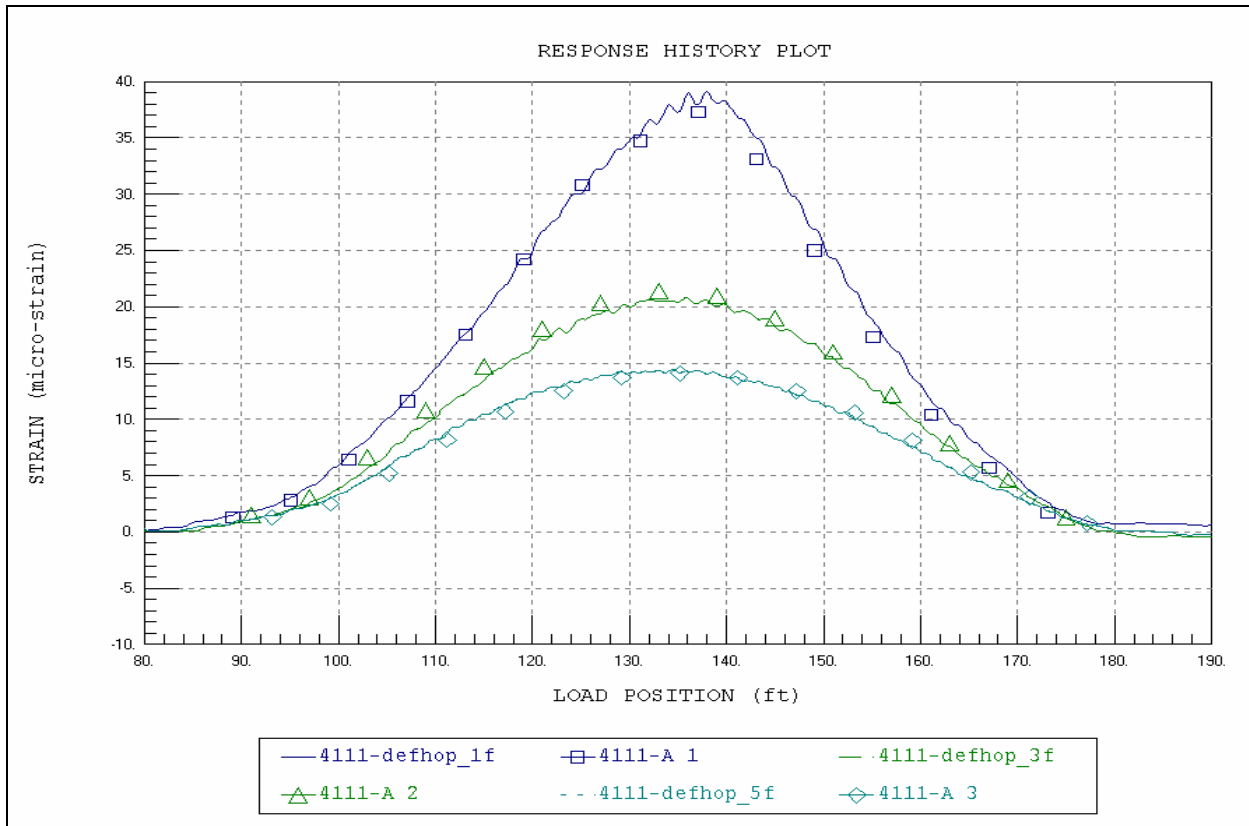


Figure 12 Span B – Beam 4 midspan.

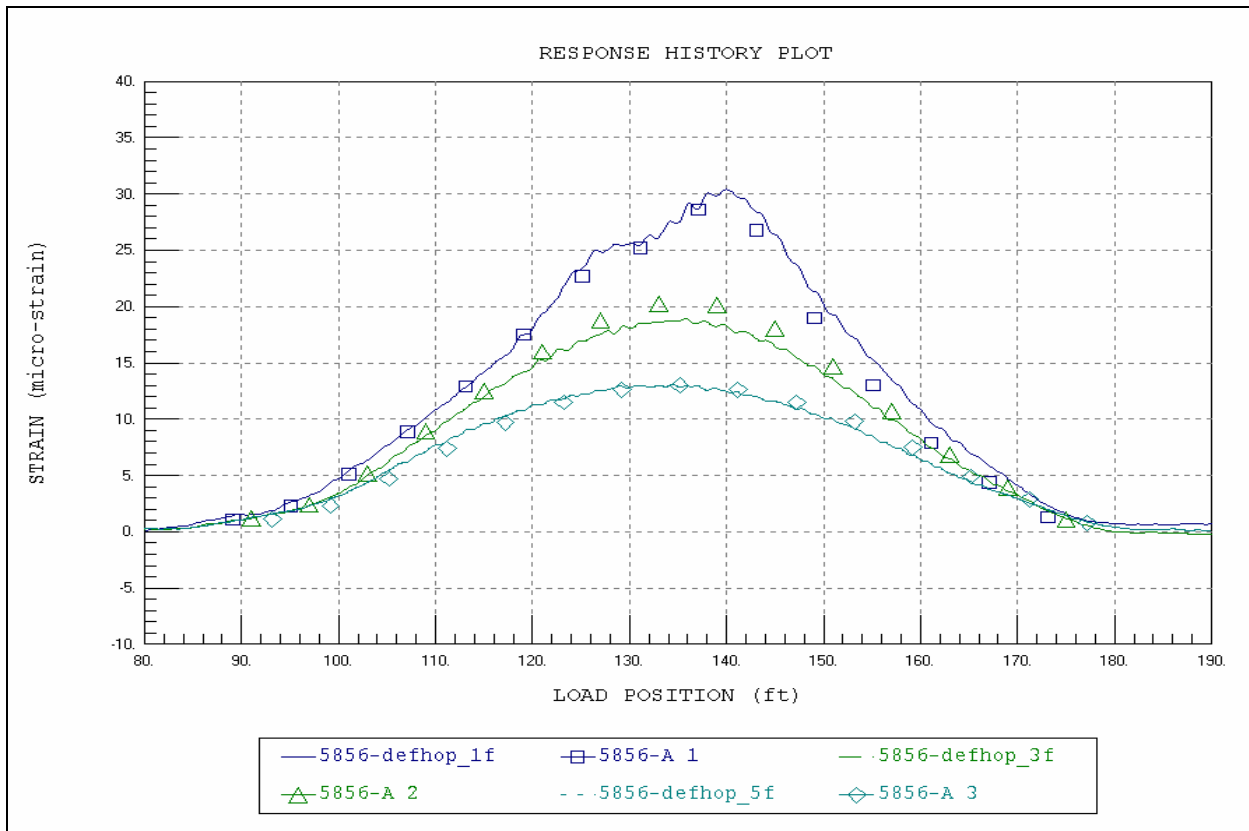


Figure 13 Span B – Beam 5 midspan.

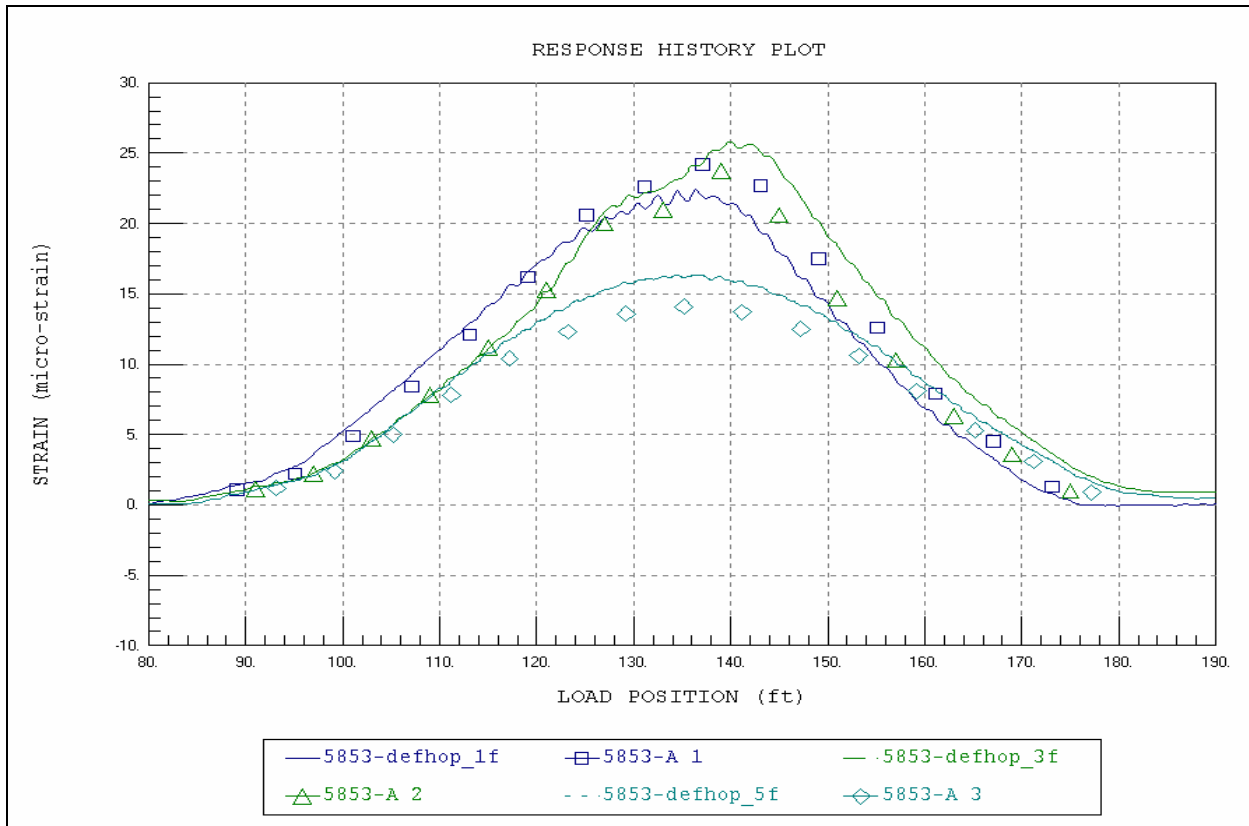


Figure 14 Span B – Beam 6 midspan.

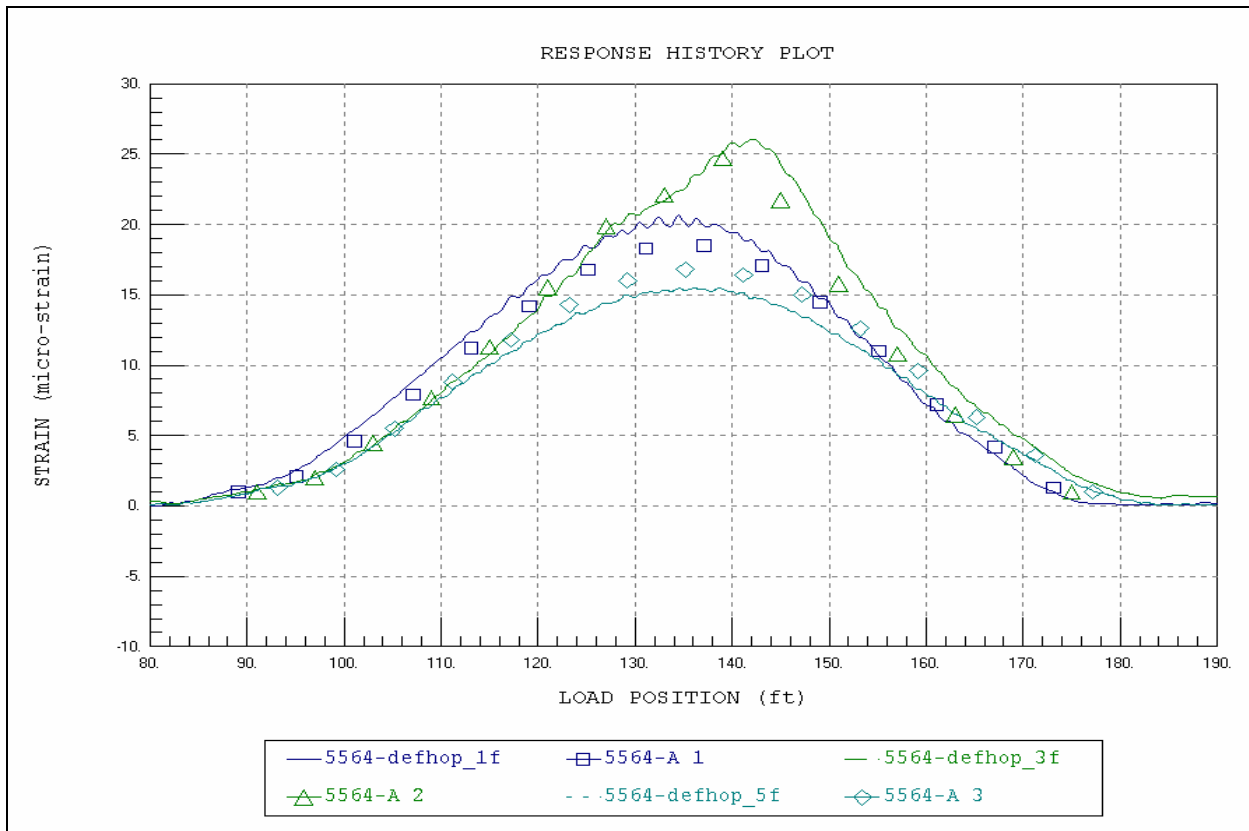


Figure 15 Span B – Beam 7 midspan.

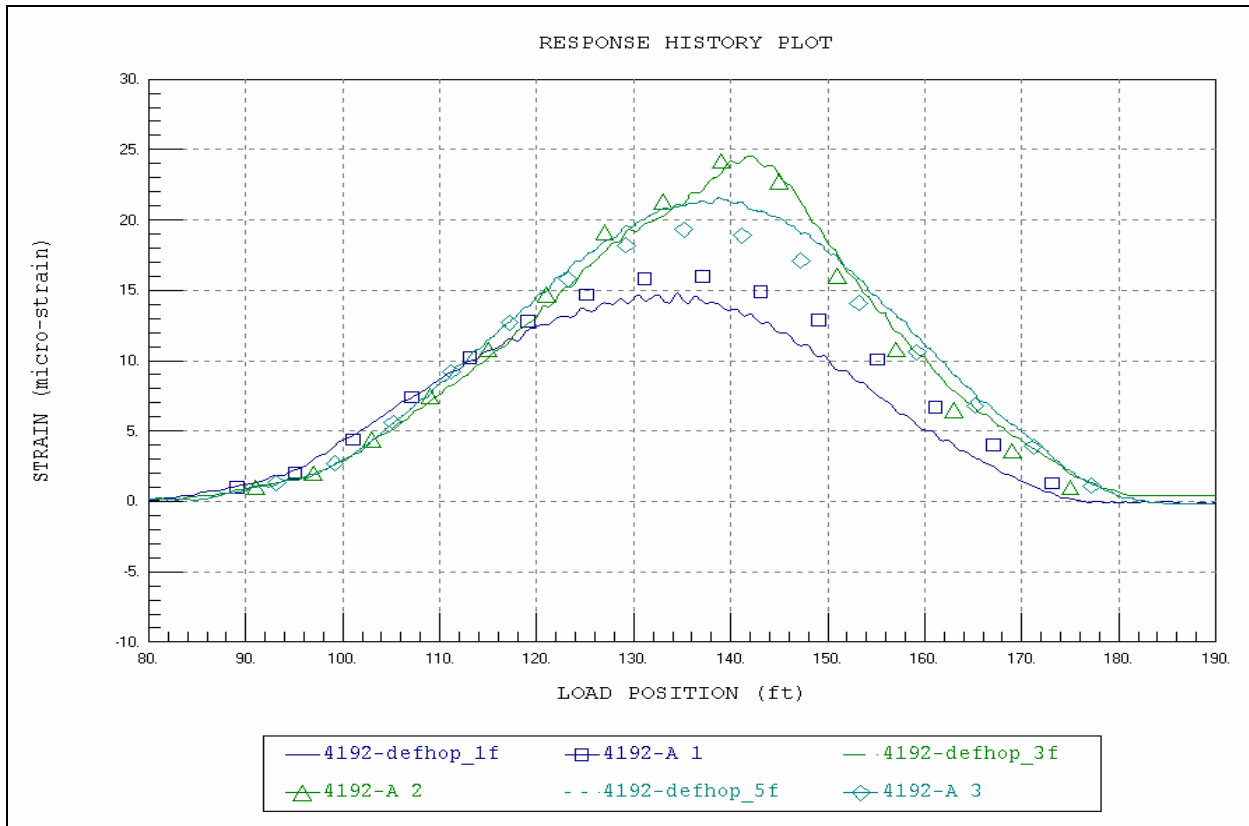


Figure 16 Span B – Beam 8 midspan.

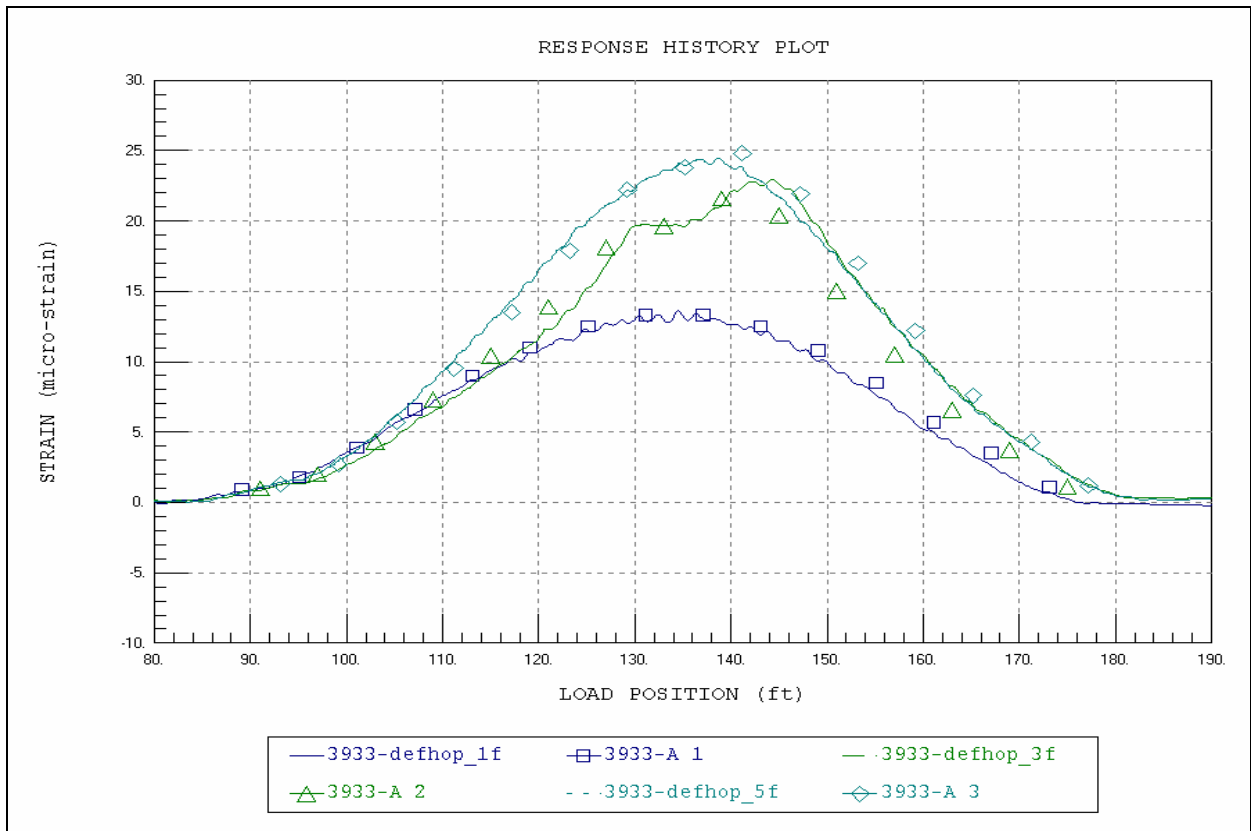


Figure 17 Span B – Beam 9 midspan.

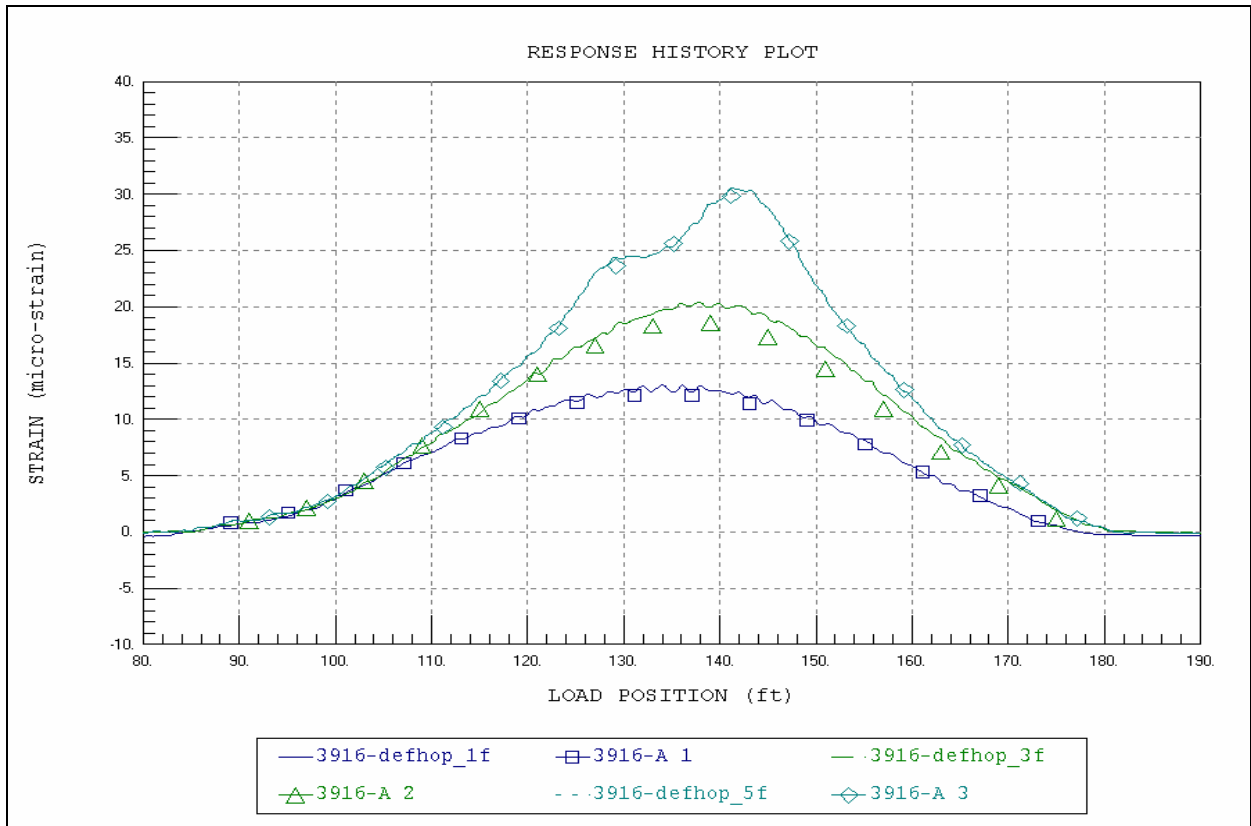


Figure 18 Span B – Beam 10 midspan.

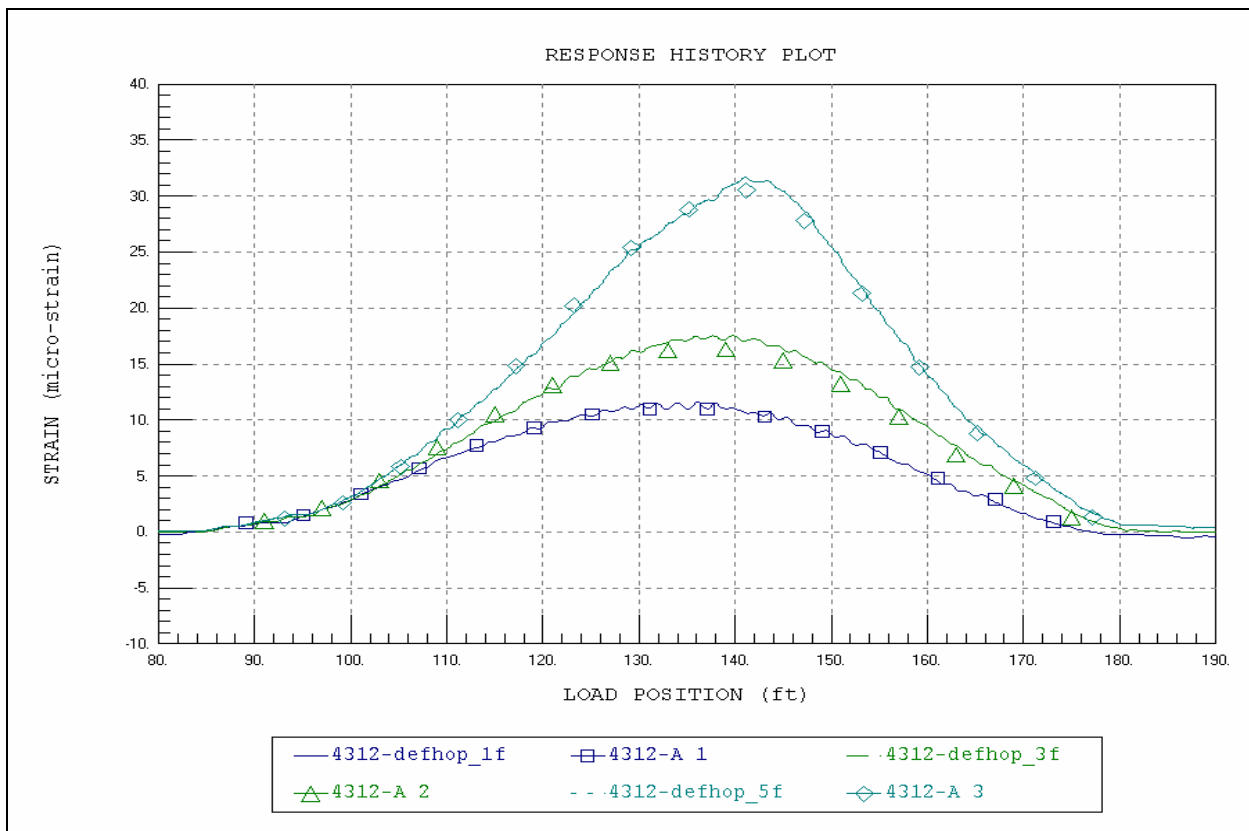


Figure 19 Span B – Beam 11 midspan.

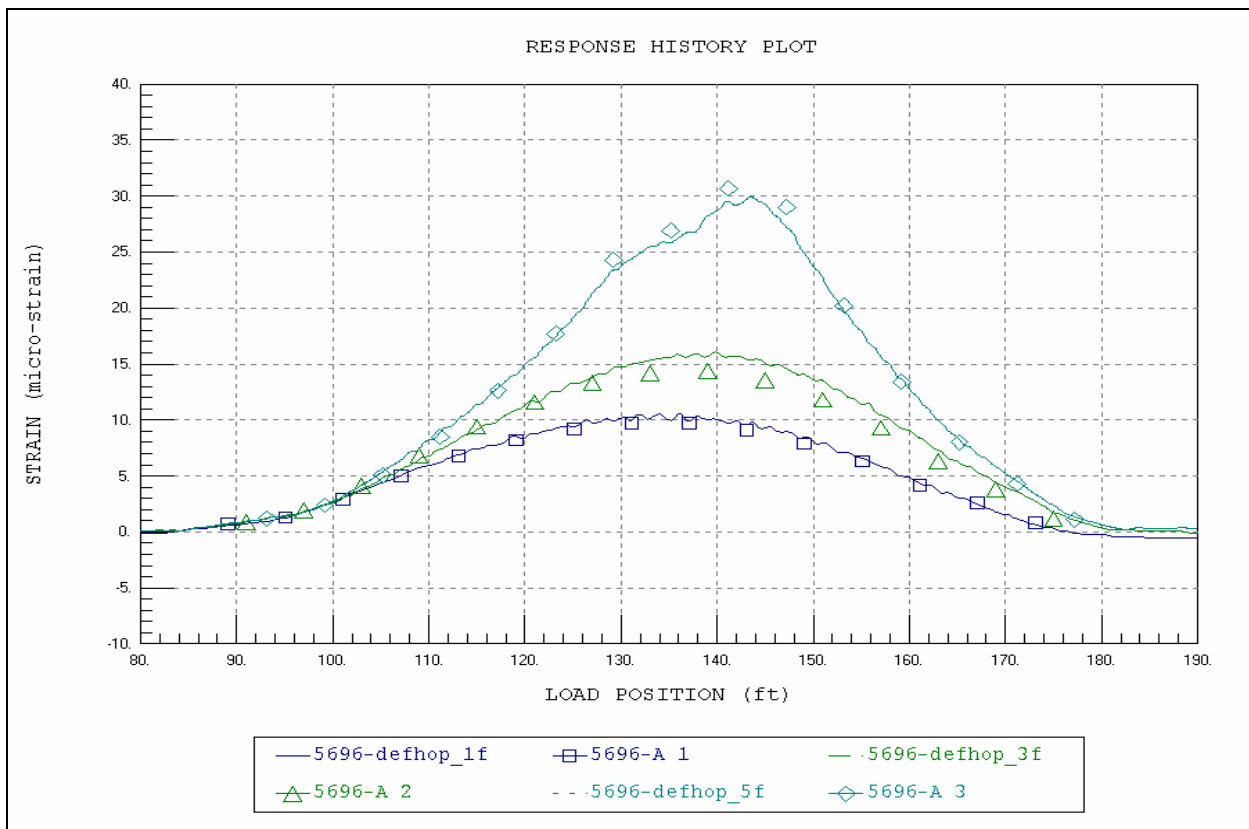


Figure 20 Span B – Beam 12 midspan.

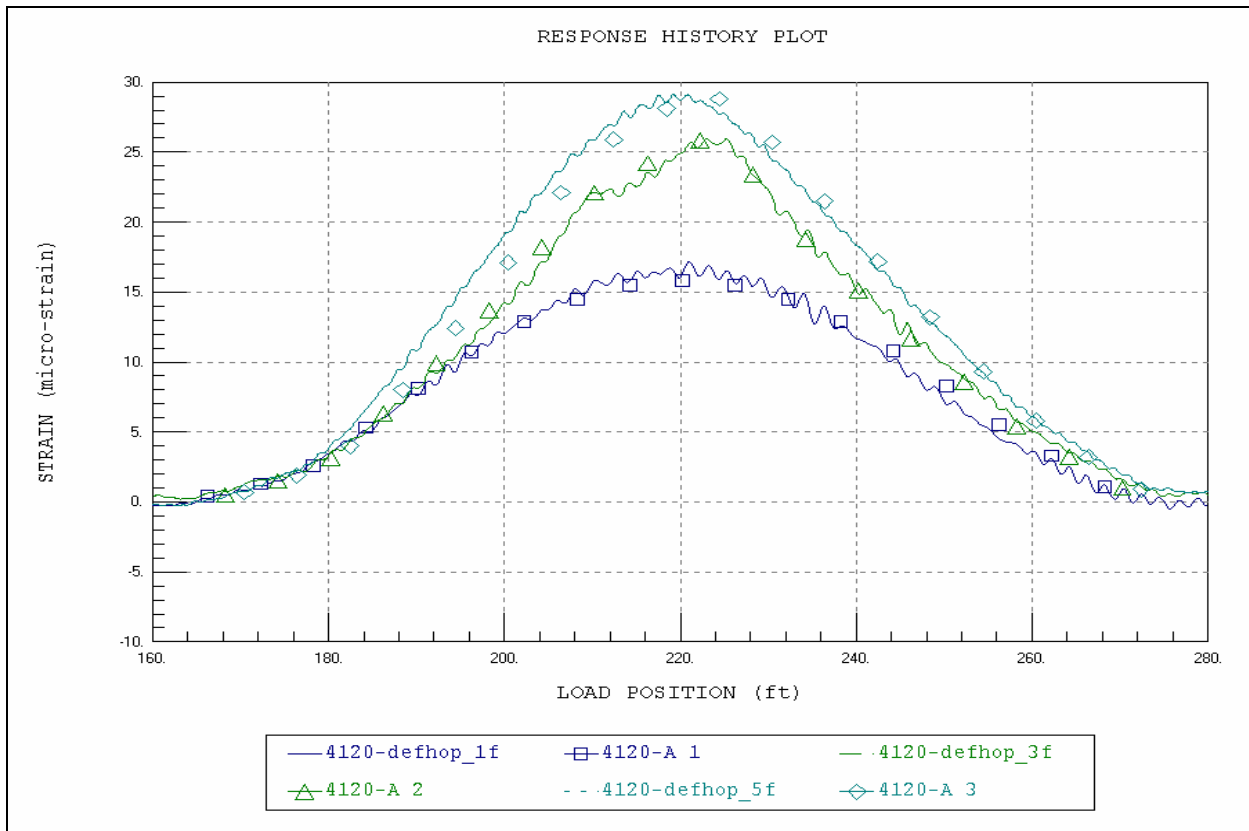


Figure 21 Span C – Beam 8 midspan.

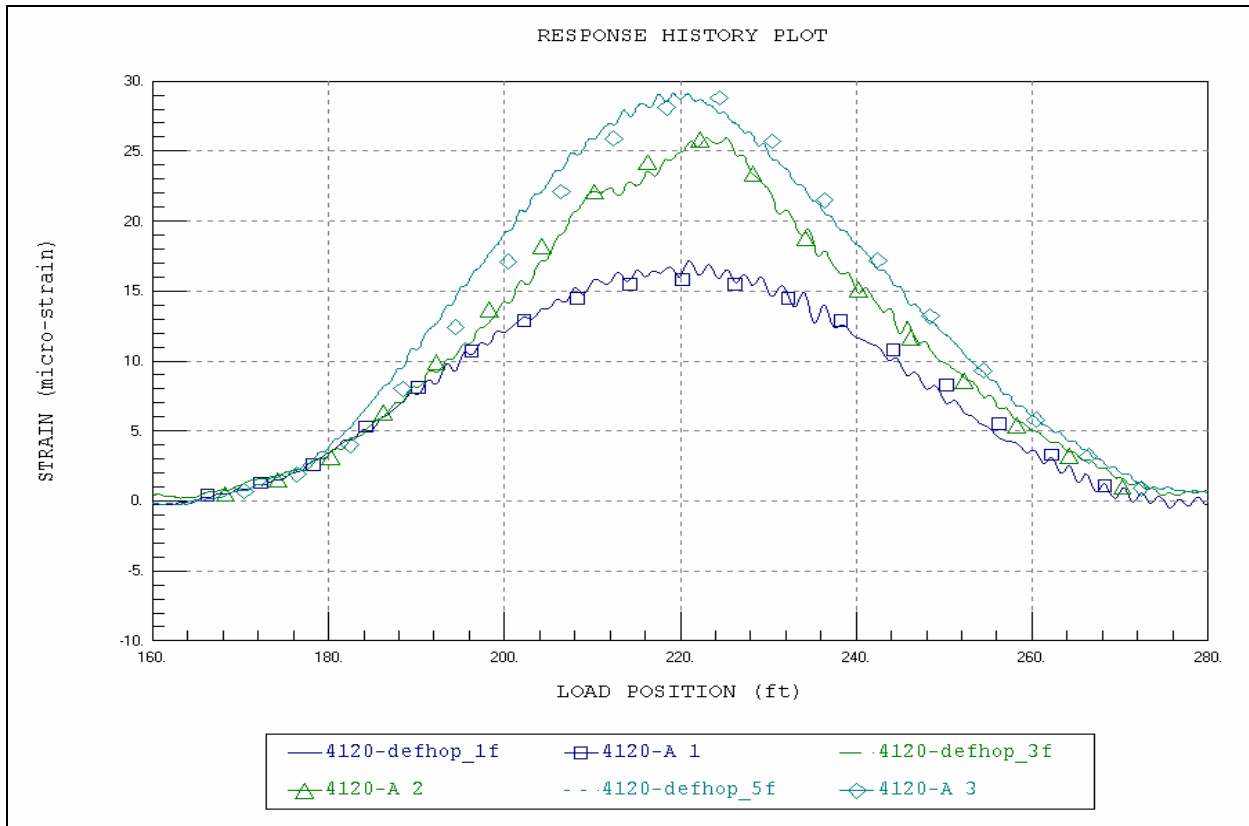


Figure 22 Span C – Beam 9 midspan.

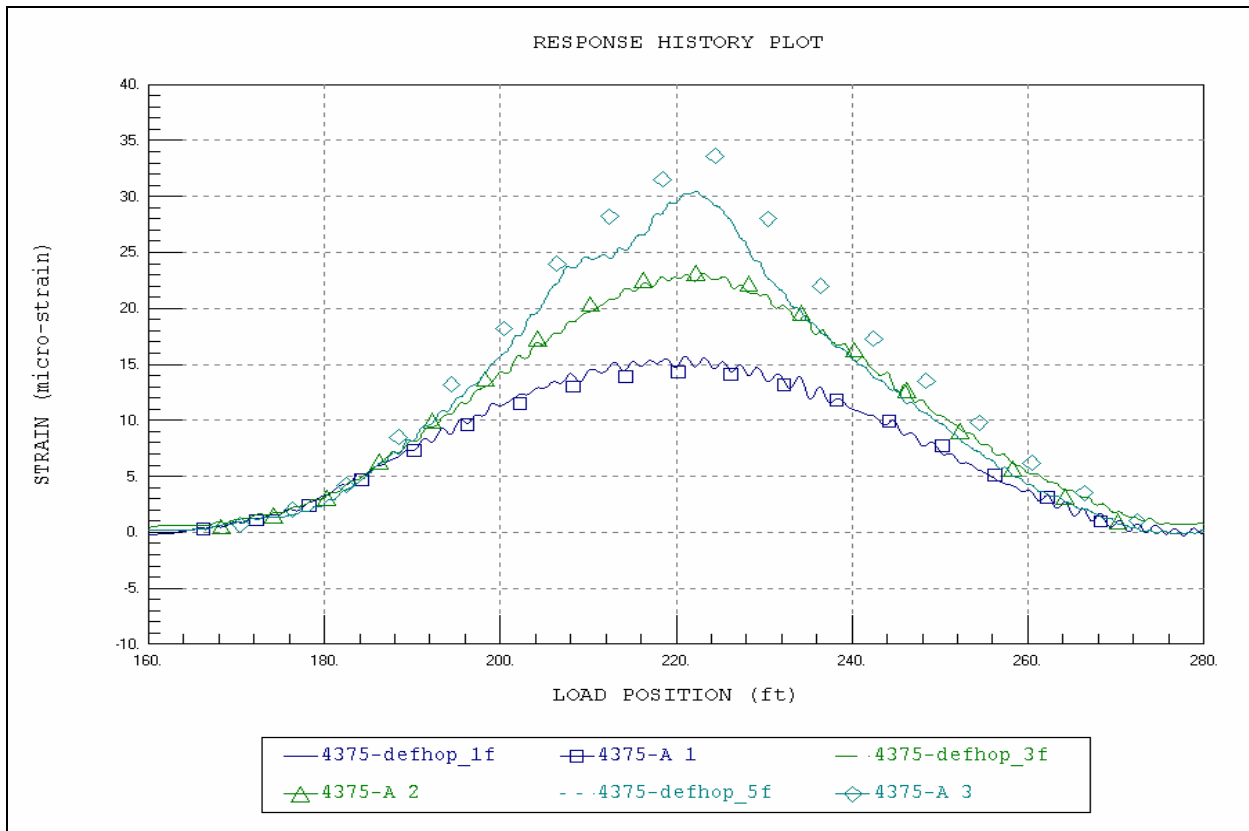


Figure 23 Span C – Beam 10 midspan.

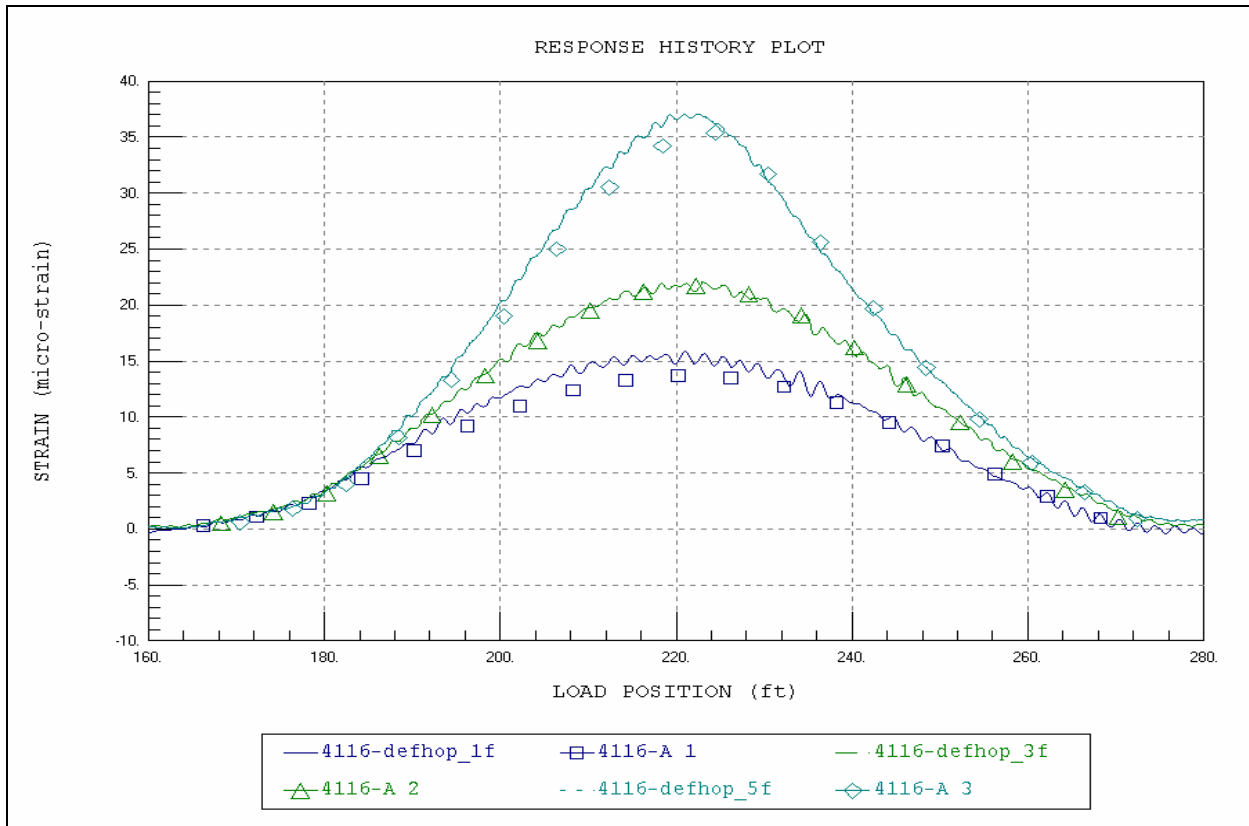


Figure 24 Span C – Beam 11 midspan.

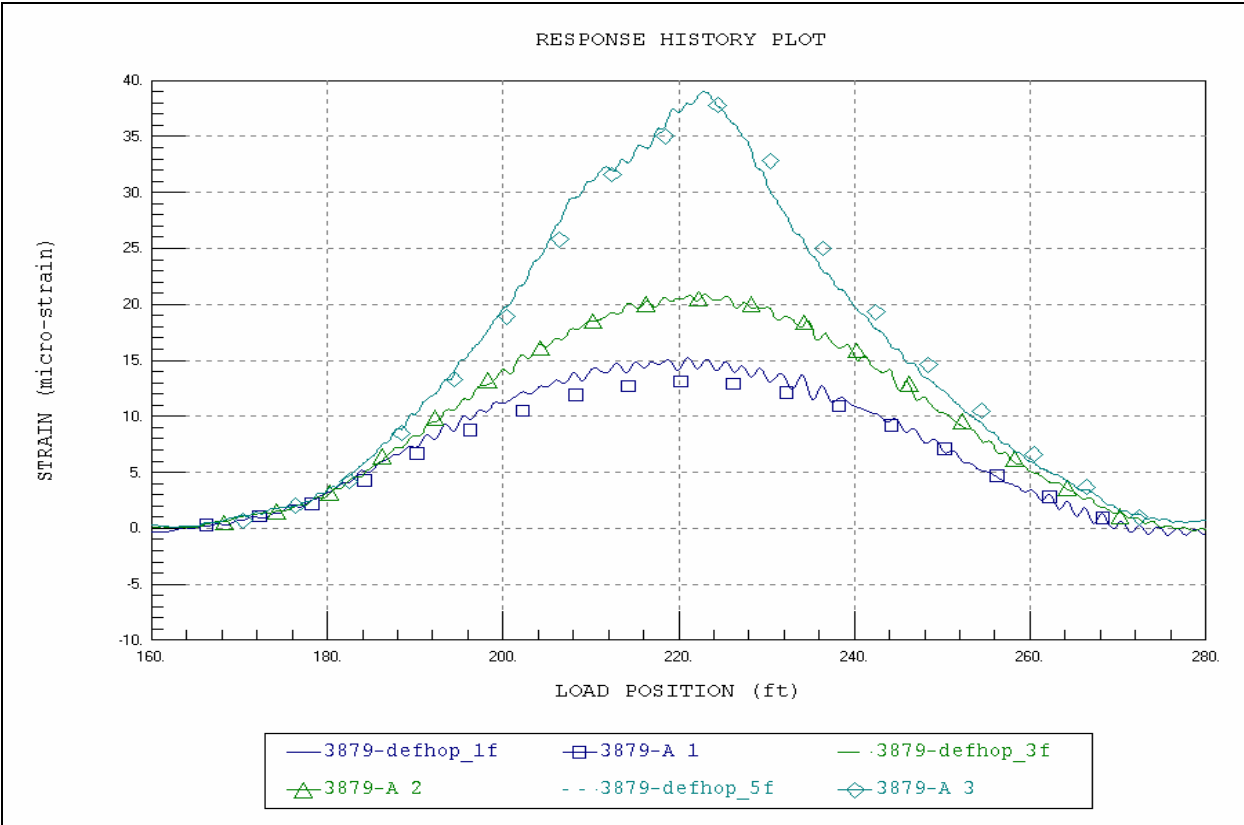


Figure 25 Span C – Beam 12 midspan.

Appendix A - Field Testing Procedures

The motivation for developing a relatively easy-to-implement field-testing system was to allow short and medium span bridges to be tested on a routine basis. Original development of the hardware was started in 1988 at the University of Colorado under a contract with the Pennsylvania Department of Transportation (PennDOT). Subsequent to that project, the Integrated Technique was refined on another study funded by the Federal Highway Administration (FHWA) in which 35 bridges located on the Interstate system throughout the country were tested and evaluated. Further refinement has been implemented over the last several years through testing and evaluating several more bridges, lock gates, and other structures.

The real key to being able to complete the field-testing quickly is the use of strain transducers (rather than standard foil strain gages) that can be attached to the structural members in just a few minutes. These sensors were originally developed for monitoring dynamic strains on foundation piles during the driving process. They have been adapted for use in structural testing through special modifications, and have 3 to 4 percent inaccuracy, and are periodically re-calibrated to NIST standards.

In addition to the strain sensors, the data acquisition hardware has been designed specifically for field use through the use of rugged cables and military-style connectors. This allows quick assembly of the system and keeps bookkeeping to a minimum. The analog-to-digital converter (A/D) is an off-the-shelf-unit, but all signal conditioning, amplification, and balancing hardware has been specially designed for structural testing. The test software has been written to allow easy configuration (test length, etc.) and operation. The end result is a system that can be used by people other than computer experts or electrical engineers. Other enhancements include the use of an automatic remote-control position indicator. The Autoclicker, a device that electronically counts wheel revolutions, is mounted on the test vehicle over one of the wheels. As the test vehicle crosses the structure along the preset path, a communication radio sends a signal to the strain measurement system that receives it and puts a mark in the data. This allows the field strains to be compared to analytical strains as a function of vehicle position, not only as a function of time.

The use of a moving load as opposed to placing the truck at discrete locations has two major benefits. First, the testing can be completed much quicker, meaning there is less impact on traffic. Second, and more importantly, much more information can be obtained (both quantitative and qualitative). Discontinuities or unusual responses in the strain histories, which are often signs of distress, can be easily detected. Since the load position is monitored as well, it is easy to determine what loading conditions cause the observed effects. If readings are recorded only at discreet truck locations, the risk of losing information between the points is great. The advantages of continuous readings have been proven over and over again.

The following list of procedures has been reproduced from the BDI Structural Testing System (STS) Operation Manual. This outline is intended to describe the general procedures used for completing a successful field test on a highway bridge using the BDI-STS. Other types of structures can be tested as well with only slight deviations from the directions given here.

Once a tentative instrumentation plan has been developed for the structure in question, the strain transducers must be attached and the STS prepared for running the test.

Attaching Strain Transducers

There are two methods for attaching the strain transducers to the structural members: C-clamping or with tabs and adhesive. For steel structures, quite often the transducers can be clamped directly to the steel flanges of rolled sections or plate girders. If significant lateral bending is assumed to be present, then one transducer may be clamped to each edge of the flange. If the transducer is to be clamped, insure that the clamp is centered over the mounting holes. In general, the transducers can be clamped directly to painted surfaces. However, if the surface being clamped to is rough or has very thick paint, it should be cleaned first with a grinder. The alternative to clamping is the tab attachment method outlined below.

1. Place two tabs in mounting jig. Place transducer over mounts and tighten the 1/4-20 nuts until they are snug (approximately 50 in-lb.). This procedure allows the tabs to be mounted without putting stress on the transducer itself. When attaching transducers to R/C members, transducer extensions are used to obtain a longer gage length. In this case the extension is bolted to one end of the transducer and the tabs are bolted to the free ends of the transducer and the extension.
2. Mark the centerline of the transducer location on the structure. Place marks 1-1/2 inches on either side of the centerline and using a hand grinder, remove paint or scale from these areas. If attaching to concrete, lightly grind the surface to remove any scale. If the paint is quite thick, use a chisel to remove most of it before grinding.
3. Very lightly grind the bottom of the transducer tabs to remove any oxidation or other contaminants.
4. Apply a thin line of adhesive to the bottom of each transducer tab.
5. Spray each tab and the contact area on the structural member with the adhesive accelerator.
6. Mount transducer in its proper location and apply a light force to the tabs (not the center of the transducer) for approximately 10 seconds.

If the above steps are followed, it should be possible to mount each transducer in approximately five minutes. When the test is complete, *carefully* loosen the 1/4-20 nuts from the tabs and remove transducer. If one is not careful, the tab will pop loose from the structure and the transducer may be damaged. Use vice grips to remove the tabs from the structure.

Assembly of System

Once the transducers have been mounted, they should be connected into an STS unit. The STS units should be placed near the transducer locations in such a manner to allow four transducers to be plugged in. Each STS unit can be easily clamped to the

bridge girders. If the structure is concrete and no flanges are available to set the STS units on, transducer tabs glued to the structure and plastic zip-ties or small wire can be used to hold them up. Since the transducers will identify themselves to the system, there is no special order that they must follow. The only information that must be recorded is the transducer serial number and its location on the structure. Large cables are provided which can be connected between the STS units. The maximum length between STS units is 50ft (15m). If several gages are in close proximity to each other, then the STS units can be plugged directly to each other without the use of a cable. All connectors will "click" when the connection has been completed properly.

Once all of the STS units have been connected in series, one cable must be run and connected to the power supply located near the PC. Connect the 9-pin serial cable between the computer and the power supply. The position indicator is then assembled and the system connected to a power source (either 12VDC or 120-240AC). The system is now ready to acquire data.

Performing Load Test

The general testing sequence is as follows:

1. Transducers are mounted and the system is connected together and turned on.
2. The deck is marked out for each truck pass. Locate the point on the deck directly above the first bearing for one of the fascia beams. If the bridge is skewed, the first point encountered from the direction of travel is used and an imaginary line extended across and normal to the roadway. All tests are started from this line. In order to track the position of the loading vehicle on the bridge during the test, an X-Y coordinate system, with the origin at the selected reference point is laid out.

In addition to monitoring the longitudinal position, the vehicle's transverse position must be known. The transverse truck position is kept uniform by first aligning the truck in the center of the lane where it would normally travel at highway speed. Next, a chalk mark is made on the deck locating the transverse location of the driver's side front wheel. By making a measurement from this mark to the reference point, the transverse ("Y") position of the truck is always known. The truck is aligned on this mark for all subsequent tests in this lane. For two lane bridges with shoulders, tests are run on the shoulder (driver's side front wheel along the white line) and in the center of each lane. If the bridge has only two lanes and very little shoulder, tests are run in the center of each lane only. If the purpose of the test is to calibrate a computer model, it is sometimes more convenient to simply use the lane lines as guides since it is easier for the driver to maintain a constant lateral position. Responses due to critical truck positions are then obtained by the analysis.

The driver is instructed that the test vehicle must be kept in the proper location on the bridge. For example, the left front wheel needs to be kept on the white line for the shoulder tests. Another important item is that the vehicles maintain a relatively constant rate of speed during the entire test. The process of converting data to a function of truck position assumes constant speed between each click mark.

Two more pieces of information are then needed: the axle weights and dimensions of the test vehicle. The driver generally provides the axle weights, after stopping at a local scale. However, a weight enforcement team can use portable scales and weigh the truck at the bridge site. Wheel base and axle width dimensions are made with a tape measure and recorded.

3. The program is started and the number of channels indicated is verified. If the number of channels indicated do not match the number of channels actually there, a malfunction has occurred and must be corrected before testing commences.
4. The transducers are initialized (zeroed out) with the Balance option. If a transducer cannot be initialized, it should be inspected to ensure that it has not been damaged.
5. The desired test length, sample rate, and output file name are selected. In general, a longer test time than the actual event is selected. For most bridge tests, a one or two-minute test length will suffice since the test can be stopped as soon as the truck crosses completely over the structure.
6. To facilitate presenting data as a function of load position, rather than time, two items describing the PI information must be defined. The starting position and PI interval distance allow the data to be plotted using position coordinates that are consistent with a numeric analysis. The starting position refers to the longitudinal position of the load vehicle in the model coordinate system when the data recording is started. The interval distance is the circumference of the tire that is being used by the Autoclicker. It is important that this information be clearly defined in the field notes.
7. If desired, the Monitor option can be used to verify transducer output during a trial test. Also, it is useful to run a Position Indicator (PI) test while in Monitor to ensure that the clicks are being received properly.
8. When all parties are ready to commence the test, the Run Test option is selected which places the system in an activated state. The Autoclicker is positioned so that the first click occurs at the starting line. This first click starts the test. The Autoclicker also puts one mark in the data for every wheel revolution. An effort should be made to get the truck across with no other traffic on the bridge. There should be no talking over the radios during the test, as a "position" will be recorded each time the microphones are activated.
9. When the test has been completed, and the system is still recording data, hit "S" to stop collecting data and finish writing the recorded data to disk. If the data files are large, they can be compressed and copied to floppy disk.
10. It is important to record the field notes very carefully. Having data without knowing where it was recorded can be worse than having no data at all. Transducer location and serial numbers must be recorded accurately. All future data handling in BDI-GRF is then accomplished by keying on the transducer number. This system has been designed to eliminate the need to track channel numbers by keeping this process in the background. However, the STS unit and the transducer's connector number are recorded in the data file if needed for future hardware evaluations.

Appendix B - Modeling and Analysis: The Integrated Approach

Introduction

In order for load testing to be a practical means of evaluating short- to medium-span bridges, it is apparent that testing procedures must be economic to implement in the field and the test results translatable into a load rating. A well-defined set of procedures must exist for the field applications as well as for the interpretation of results. An evaluation approach based on these requirements was first developed at the University of Colorado during a research project sponsored by the Pennsylvania Department of Transportation (PennDOT). Over several years, the techniques originating from this project have been refined and expanded into a complete bridge rating system.

The ultimate goal of the Integrated Approach is to obtain realistic rating values for highway bridges in a cost effective manner. This is accomplished by measuring the response behavior of the bridge due to a known load and determining the structural parameters that produce the measured responses. With the availability of field measurements, many structural parameters in the analytical model can be evaluated that are otherwise conservatively estimated or ignored entirely. Items that can be quantified through this procedure include the effects of structural geometry, effective beam stiffness, realistic support conditions, effects of parapets and other non-structural components, lateral load transfer capabilities of the deck and transverse members, and the effects of damage or deterioration. Often, bridges are rated poorly because of inaccurate representations of the structural geometry or because the material and/or cross-sectional properties of main structural elements are not well defined. A realistic rating can be obtained, however, when all of the relevant structural parameters are defined and implemented in the analysis process.

One of the most important phases of this approach is a qualitative evaluation of the raw field data. Much is learned during this step to aid in the rapid development of a representative model.

Initial Data Evaluation

The first step in structural evaluation consists of a visual inspection of the data in the form of graphic response histories. Graphic software was developed to display the raw strain data in various forms. Strain histories can be viewed in terms of time or truck position. Since strain transducers are typically placed in pairs, neutral axis measurements, curvature responses, and strain averages can also be viewed. Linearity between the responses and load magnitude can be observed by the continuity in the strain histories. Consistency in the neutral axis measurements from beam to beam and as a function of load position provides great insight into the nature of the bridge condition. The direction and relative magnitudes of flexural responses along a beam line are useful in determining if end restraints play a significant role in the response behavior. In general, the initial data inspection provides the engineer with information concerning modeling requirements and can help locate damaged areas.

Having strain measurements at two depths on each beam cross-section, flexural curvature and the location of the neutral axis can be computed directly from the field

data. Figure 26 illustrates how curvature and neutral axis values are computed from the strain measurements.

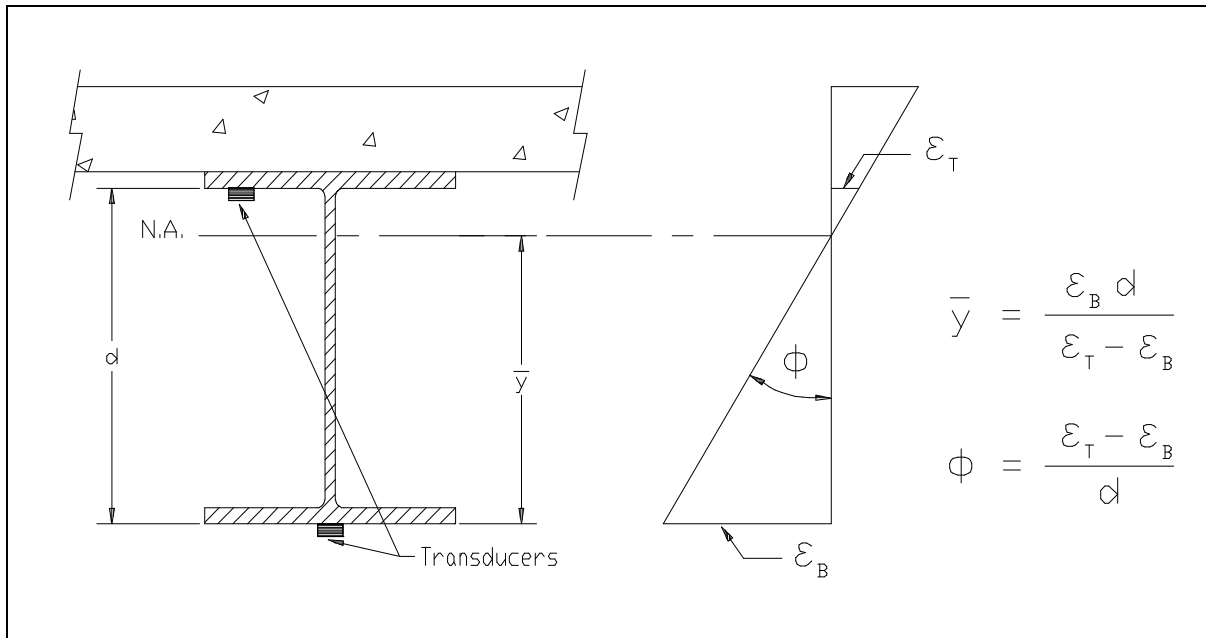


Figure 26 Illustration of Neutral Axis and Curvature Calculations

The consistency in the N.A. values between beams indicates the degree of consistency in beam stiffness. Also, the consistency of the N.A. measurement on a single beam as a function of truck position provides a good quality check for that beam. If for some reason a beam's stiffness changes with respect to the applied moment (i.e. loss of composite action or loss of effective flange width due to a deteriorated deck), it will be observed by a shift in the N.A. history.

Since strain values are translated from a function of time into a function of vehicle position on the structure and the data acquisition channel and the truck position tracked, a considerable amount of book keeping is required to perform the strain comparisons. In the past, this required manipulation of result files and spreadsheets which was tedious and a major source of error. This process is now performed automatically by the software and all of the information can be verified visually.

Finite Element Modeling and Analysis

The primary function of the load test data is to aid in the development of an accurate finite element model of the bridge. Finite element analysis is used because it provides the most general tool for evaluating various types of structures. Since a comparison of measured and computed responses is performed, it is necessary that the analysis be able to represent the actual response behavior. This requires that actual geometry and boundary conditions be realistically represented. In maintaining reasonable modeling efforts and computer run times, a certain amount of simplicity is also required, so a planar grid model is generated for most structures and linear-elastic responses are assumed. A grid of frame elements is assembled in the same geometry as the actual structure. Frame elements represent the longitudinal and transverse members of the bridge. The load transfer characteristics of the deck are provided by attaching plate elements to the grid. When end restraints are determined to be present, elastic spring

elements having both translational and rotational stiffness terms are inserted at the support locations.

Loads are applied in a manner similar to the actual load test. A model of the test truck, defined by a two-dimensional group of point loads, is placed on the structure model at discrete locations along the same path that the test truck followed during the load test. Gage locations identical to those in the field are also defined on the structure model so that strains can be computed at the same locations under the same loading conditions.

Model Correlation and Parameter Modifications

The accuracy of the model is determined numerically by the analysis using several statistical relationships and through visual comparison of the strain histories. The numeric accuracy values are useful in evaluating the effect of any changes to the model, where as the graphical representations provide the engineer with the best perception for why the model is responding differently than the measurements indicate. Member properties that cannot be accurately defined by conventional methods or directly from the field data are evaluated by comparing the computed strains with the measured strains. These properties are defined as variable and are evaluated such that the best correlation between the two sets of data is obtained. It is the engineer's responsibility to determine which parameters need to be refined and to assign realistic upper and lower limits to each parameter. The evaluation of the member property is accomplished with the aid of a parameter identification process (optimizer) built into the analysis. In short, the process consists of an iterative procedure of analysis, data comparison, and parameter modification. It is important to note that the optimization process is merely a tool to help evaluate various modeling parameters. The process works best when the number of parameters is minimized and reasonable initial values are used.

During the optimization process, various error values are computed by the analysis program that provide quantitative measure of the model accuracy and improvement. The error is quantified in four different ways, each providing a different perspective of the model's ability to represent the actual structure; an absolute error, a percent error, a scale error and a correlation coefficient.

The **absolute error** is computed from the absolute sum of the strain differences. Algebraic differences between the measured and theoretical strains are computed at each gage location for each truck position used in the analysis, therefore, several hundred strain comparisons are generally used in this calculation. This quantity is typically used to determine the relative accuracy from one model to the next and to evaluate the effect of various structural parameters. It is used by the optimization algorithm as the objective function to minimize. Because the absolute error is in terms of micro-strain ($m\epsilon$) the value can vary significantly depending on the magnitude of the strains, the number of gages and number of different loading scenarios. For this reason, it has little conceptual value except for determining the relative improvement of a particular model.

A **percent error** is calculated to provide a better qualitative measure of accuracy. It is computed as the sum of the strain differences squared divided by the sum of the measured strains squared. The terms are squared so that error values of different sign will not cancel each other out, and to put more emphasis on the areas with higher strain

magnitudes. A model with acceptable accuracy will usually have a percent error of less than 10%.

The **scale error** is similar to the percent error except that it is based on the maximum error from each gage divided by the maximum strain value from each gage. This number is useful because it is based only on strain measurements recorded when the loading vehicle is in the vicinity of each gage. Depending on the geometry of the structure, the number of truck positions, and various other factors, many of the strain readings are essentially negligible. This error function uses only the most relevant measurement from each gage.

Another useful quantity is the **correlation coefficient** which is a measure of the linearity between the measured and computed data. This value determines how well the shape of the computed response histories match the measured responses. The correlation coefficient can have a value between 1.0 (indicating a perfect linear relationship) and -1.0 (exact opposite linear relationship). A good model will generally have a correlation coefficient greater than 0.90. A poor correlation coefficient is usually an indication that a major error in the modeling process has occurred. This is generally caused by poor representations of the boundary conditions or the loads were applied incorrectly (i.e. truck traveling in wrong direction).

The following table contains the equations used to compute each of the statistical error values:

Table 11. Error Functions

| ERROR FUNCTION | EQUATION |
|-------------------------|---|
| Absolute Error | $\sum \epsilon_m - \epsilon_c $ |
| Percent Error | $\sum (\epsilon_m - \epsilon_c)^2 / \sum (\epsilon_m)^2$ |
| Scale Error | $\frac{\sum \max \epsilon_m - \epsilon_c _{gage}}{\sum \max \epsilon_m _{gage}}$ |
| Correlation Coefficient | $\frac{\sum (\epsilon_m - \bar{\epsilon}_m)(\epsilon_c - \bar{\epsilon}_c)}{\sum \sqrt{(\epsilon_m - \bar{\epsilon}_m)^2 (\epsilon_c - \bar{\epsilon}_c)^2}}$ |

In addition to the numerical comparisons made by the program, periodic visual comparisons of the response histories are made to obtain a conceptual measure of accuracy. Again, engineering judgment is essential in determining which parameters should be adjusted so as to obtain the most accurate model. The selection of adjustable parameters is performed by determining what properties have a significant effect on the strain comparison and determining which values cannot be accurately estimated through conventional engineering procedures. Experience in examining the data comparisons is helpful, however, two general rules apply concerning model refinement. When the shapes of the computed response histories are similar to the measured strain records but the

magnitudes are incorrect this implies that member stiffnesses must be adjusted. When the shapes of the computed and measured response histories are not very similar then the boundary conditions or the structural geometry are not well represented and must be refined.

In some cases, an accurate model cannot be obtained, particularly when the responses are observed to be non-linear with load position. Even then, a great deal can be learned about the structure and intelligent evaluation decisions can be made.

Appendix C - Load Rating Procedures

For borderline bridges (those that calculations indicate a posting is required), the primary drawback to conventional bridge rating is an oversimplified procedure for estimating the load applied to a given beam (i.e. wheel load distribution factors) and a poor representation of the beam itself. Due to lack of information and the need for conservatism, material and cross-section properties are generally over-estimated and beam end supports are assumed to be simple when in fact even relatively simple beam bearings have a substantial effect on the midspan moments. Inaccuracies associated with conservative assumptions are compounded with complex framing geometries. From an analysis standpoint, the goal here is to generate a model of the structure that is capable of reproducing the measured strains. Decisions concerning load rating are then based on the performance of the model once it is proven to be accurate.

The main purpose for obtaining an accurate model is to evaluate how the bridge will respond when standard design loads, rating vehicles or permit loads are applied to the structure. Since load testing is generally not performed with all of the vehicles of interest, an analysis must be performed to determine load-rating factors for each truck type. Load rating is accomplished by applying the desired rating loads to the model and computing the stresses on the primary members. Rating factors are computed using the equation specified in the AASHTO Manual for Condition Evaluation of Bridges - see Equation (1).

It is important to understand that diagnostic load testing and the integrated approach are most applicable to obtaining Inventory (service load) rating values. This is because it is assumed that all of the measured and computed responses are linear with respect to load. The integrated approach is an excellent method for estimating service load stress values but it generally provides little additional information regarding the ultimate strength of particular structural members. Therefore, operating rating values must be computed using conventional assumptions regarding member capacity. This limitation of the integrated approach is not viewed as a serious concern, however, because load responses should never be permitted to reach the inelastic range.

Operating and/or Load Factor rating values must also be computed to ensure a factor of safety between the ultimate strength and the maximum allowed service loads. The safety to the public is of vital importance but as long as load limits are imposed such that the structure is not damaged then safety is no longer an issue.

Following is an outline describing how field data is used to help in developing a load rating for the superstructure. These procedures will only complement the rating process, and must be used with due consideration to the substructure and inspection reports.

1. **Preliminary Investigation:** Verification of linear and elastic behavior through continuity of strain histories, locate neutral axis of flexural members, detect moment resistance at beam supports, qualitatively evaluate behavior.

2. **Develop representative model:** Use graphic pre-processors to represent the actual geometry of the structure, including span lengths, girder spacing, skew, transverse members, and deck. Identify gage locations on model identical to those applied in the field.
3. **Simulate load test on computer model:** Generate 2-dimensional model of test vehicle and apply to structure model at discrete positions along same paths defined during field tests. Perform analysis and compute strains at gage location for each truck position.
4. **Compare measured and initial computed strain values:** Various global and local error values at each gage location are computed and visual comparisons made with post-processor.
5. **Evaluate modeling parameters:** Improve model based on data comparisons. Engineering judgment and experience is required to determine which variables are to be modified. A combination of direct evaluation techniques and parameter optimization are used to obtain a realistic model. General rules have been defined to simplify this operation.
6. **Model evaluation:** In some cases it is not desirable to rely on secondary stiffening effects if it is likely they will not be effective at higher load levels. It is beneficial, though, to quantify their effects on the structural response so that a representative computer model can be obtained. The stiffening effects that are deemed unreliable can be eliminated from the model prior to the computation of rating factors. For instance, if a non-composite bridge is exhibiting composite behavior, then it can conservatively be ignored for rating purposes. However, if it has been in service for 50 years and it is still behaving compositely, chances are that very heavy loads have crossed over it and any bond-breaking would have already occurred. Therefore, probably some level of composite behavior can be relied upon. When unintended composite action is allowed in the rating, additional load limits should be computed based on an allowable shear stress between the steel and concrete and an ultimate load of the non-composite structure.
7. **Perform load rating:** Apply HS-20 and/or other standard design, rating and permit loads to the calibrated model. Rating and posting load configuration recommended by AASHTO are shown in Figure 27. The same rating equation specified by the **AASHTO - Manual for the Condition Evaluation of Bridges** is applied:

$$RF = \frac{C - A_1 D}{A_2 L(1 + I)} \quad (1)$$

where:

- RF = Rating Factor for individual member.
- C = Member Capacity.
- D = Dead-Load effect.
- L = Live-Load effect.
- A_1 = Factor applied to dead-load.
- A_2 = Factor applied to live-load.
- I = Impact effect, either AASHTO or measured.

The only difference between this rating technique and standard beam rating programs is that a more realistic model is used to determine the dead-load and live-load effects. Two-dimensional loading techniques are applied because wheel load distribution factors are not applicable to a planar model. Stress envelopes are generated for several truck paths, envelopes for paths separated by normal lane widths are combined to determine multiple lane loading effects.

8. **Consider other factors:** Other factors such as the condition of the deck and/or substructure, traffic volume, and other information in the inspection report should be taken into consideration and the rating factors adjusted accordingly.

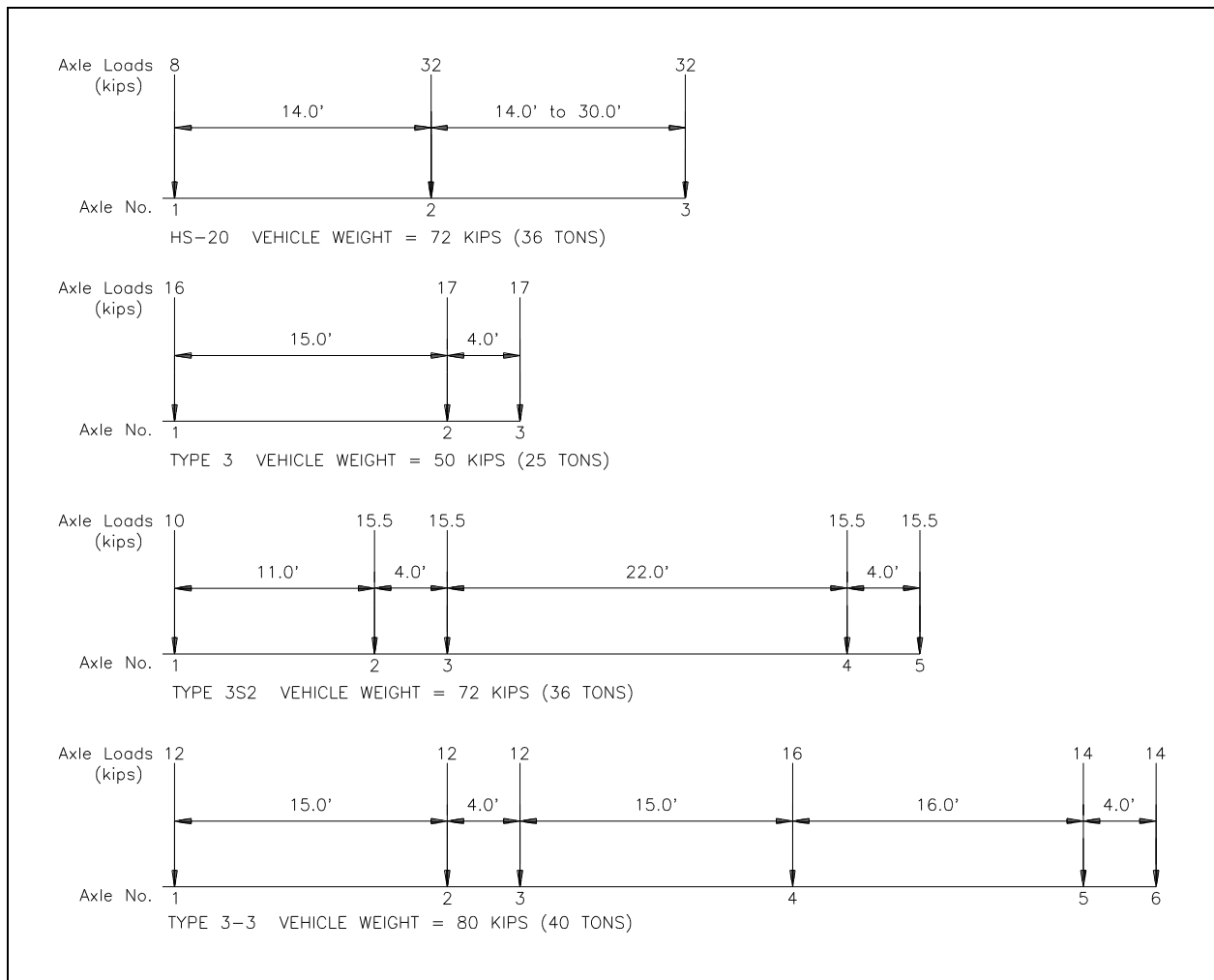


Figure 27 AASHTO rating and posting load configurations.

Appendix D - References

AASHTO (1989). "Standard Specification for Highway Bridges." Washington, D.C.

AASHTO, (1994). "Manual for the Condition Evaluation of Bridges", Washington, D.C.

Commander, B., (1989). "An Improved Method of Bridge Evaluation: Comparison of Field Test Results with Computer Analysis." Master Thesis, University of Colorado, Boulder, CO.

Gerstle, K.H., and Ackroyd, M.H. (1990). "*Behavior and Design of Flexibly-Connected Building Frames*." Engineering Journal, AISC, 27(1), 22-29.

Goble, G., Schulz, J., and Commander, B. (1992). "Load Prediction and Structural Response." Final Report, FHWA DTFH61-88-C-00053, University of Colorado, Boulder, CO.

Lichtenstein, A.G. (1995). "Bridge Rating Through Nondestructive Load Testing." Technical Report, NCHRP Project 12-28(13)A.

Schulz, J.L. (1989). "Development of a Digital Strain Measurement System for Highway Bridge Testing." Masters Thesis, University of Colorado, Boulder, CO.

Schulz, J.L. (1993). "In Search of Better Load Ratings." *Civil Engineering*, ASCE 63(9), 62-65.